2009

Optimal area and impedance allocation for maximizing yield and enhancing performance in dual string DACs

Thu Thi Anh Duong
Iowa State University

Optimal area and impedance allocation for maximizing yield and enhancing performance in dual string DACs

by

Thu Thi-Anh Duong

A thesis submitted to the graduate faculty

in partial fulfillment of the requirements for the degree of

MASTER OF SCIENCE

Major: Electrical Engineering

Program of Study Committee:
Randall L. Geiger, Major Professor
Chen Degang
Tien Nguyen

Iowa State University

Ames, Iowa

2009

TABLE OF CONTENTS

LIST OF FIGURES

LIST OF TABLES

ABSTRACT

The relationships between yield, area, and impedance distribution in 3 different types of dual-string DACs are developed. Optimal area allocation and impedance distribution strategies for maximizing yield and enhancing performance are introduced. Simulation results show that a factor of 2 or more reduction in area for a given yield is possible if typical area/impedance allocations are replaced with an optimal area/impedance allocation.

CHAPTER 1. INTRODUCTION

Dual-ladder resistor string digital analog converters (DACs), which incorporate fine string least significant bit (LSB) ladders in parallel between two successive coarse ladder taps are widely used in industry [Boylston, L. E. et al. (2002), Pelgrom, M. J. M. (1990), Maloberti, F. et al. (1996), Rivoir, R. et al. (1997)]. When properly designed, the dual-ladder structures inherit most of the advantages of a string DAC such as monotonicity, speed, and versatility [Boylston, L. E. et al.]. The major advantage of the dual-ladder DACs with a reduced number of resistors in the coarse ladder comes at the layout stage where layout complexity can be reduced since a common centroid layout of the coarse string resistors will effectively cancel linear gradient effects [Maloberti, F. et al. (1996)] for the entire DAC.

It is well known that layout contributes a very important part to the linearity performance of the DAC. Different layout approaches provide different integral Non-Linearity (INL) performance. Conventional wisdom suggests that the value of the coarse string resistors should be small and the area for the coarse string resistors should be large for a properly designed dual-ladder DAC [Plassche, R. van de (2003)]. Although the area allocation in the dual-ladder DAC used in [Pelgrom, M. J. M. (1990)] was not given, a die photograph shows that the total area for the fine resistor string was approximately 7 times that for the coarse string while the ratio of the total series fine resistance to the total series coarse resistances was about 38. Other research results are based upon the assumption that the unity fine resistor values are a power of 2 times the unit coarse resistor values [Maloberti, F. et al. (1996)]. Surprisingly, authors discussing these heuristic approaches to allocation of area and impedance values between the coarse and fine resistors in the strings are silent about

the issue of optimality. An optimal strategy for maximizing INL yield in dual-string DACs requires allocation of silicon area and impedances of the coarse ladder and the fine ladder strings to minimize the effects random local variations in the sheet resistance on the INL performance. Unfortunately, there is a little research suggesting how areas and impedances related to the linear performance of the dual ladder DAC when mismatch of resistors is considered. As a result, many engineers allocate excessive area to achieve a required yield or obtain a poor yield to meet a fixed area target without realizing that the excessive area or the yield loss is often due to non-optimal allocation of area and impedance between the string ladders. Although INL yield can be improved by increasing area in either the coarse or fine ladder, it this is done in a non-optimal way, it will result in an increase in die costs and increases in parasitic capacitors which will reduce the speed and thus limit the high frequency performance of the circuit.

As with any string DAC, the linearity performance of the dual-string architecture is mainly limited by the presence of process and gradient effects and the random mismatch of the resistors in the ladders. If the areas of the resistors are not too large, the gradient will be nearly linear (first-order). The effects of first-order gradients on ratio matching can be canceled or minimized by appropriate placement, segmentation and the use of common-centroid layout methods [Hastings, A. (2000)].

If gradient effects are cancelled, the random mismatch of the resistors in the ladders becomes the domain contributor to the nonlinearity performance of this architecture. This mismatch is usually dominated by the local random variations in the sheet resistance throughout the body of the resistors. The resultant random variations in the individual resistors are usually modeled as a Gaussian random variable. It is well-known that

maximizing the resistor area is effective for minimizing the effects of local random variations on the overall mismatch of the resistors [Pelgrom, M. J. M. (1990)]. Thus, designers routinely mark tradeoffs between area and matching accuracy.

In this work, linearity performance tradeoffs between area in the coarse string and area in the fine string and between the resistance values in the coarse string and the resistance values in the fine string are discussed. The issue of optimal area and impedance allocation strategies for minimizing the INL is addressed.

CHAPTER 2. ALLOCATING AREAS AND IMPEDANCES

In this chapter, three different types of dual – ladder strings are discussed. The concept of how area and impedance allocation affects the performance of resistor strings can be more easily described by considering first a much simpler circuit comprised of two resistors in parallel. This is the topic of the following section.

2.1 The INL variance of two resistors in parallel

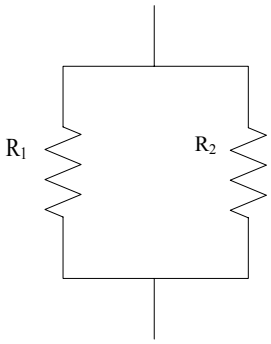

Figure 1. Parrallel Resistors

A simple circuit comprised of two parallel resistors is discussed in this section. This circuit is useful for providing insight into the tradeoffs between area, impedance values and performance of resistor circuits that are plagued by local random variations in the sheet resistance. The normalized variance of the equivalent resistance of the two parallel resistors will be characterized in detailed. The results will provide insight into the analysis and optimization of the integral nonlinearity (INL) of the dual ladder resistor string that is discussed in the next section.

Consider the two resistors shown in the Figure 1 where the resistance values and active layout areas are R_1, R_2, A_1 and A_2. The equivalent resistance of the parallel

combination is $R = \frac{R_1 R_2}{R_1 + R_2}$. For notational convenience, the variables u and v are defined by the expressions

$$u = \frac{A_1}{A_{TOT}} \tag{1}$$

$$v = \frac{R}{R_1} \tag{2}$$

where A_{TOT} is the total area of two resistors. It is apparent that (u,v) are restricted to the open unit square in the u-v plane.

If it is assumed that only linear gradient affects are present in the layout of the two resistors and if a common centroid layout method is used, linear gradient effects in are cancelled and each of the resistors can be decomposed into the sum of the nominal resistance R_N and a component due to the local random variation in the sheet resistance R_R. Mathematically, for each resistor, this relationship can be repressed as $R_i = R_{iN} + R_{iR}$ where R_{iN} is the nominal value of the resistance at the geometric centroid of the layout and R_{iR} is the random component of R_i. The random components of R_1 and R_2 are generally assumed to be uncorrelated. For useful resistors in matching-critical applications, it can be assumed the R_{iR} is small compared to R_{iN}. With this notation, the equivalent resistance can be expressed as

$$R = \frac{\left(R_{1N} + R_{1R}\right)\left(R_{2N} + R_{2R}\right)}{\left(R_{1N} + R_{1R} + R_{2N} + R_{2R}\right)} \tag{3}$$

By factoring out the nominal value of resistors, (3) can be rewritten as:

$$R = \frac{R_{1N}R_{2N}}{(R_{1N}+R_{2N})} \frac{\left(1+\frac{R_{1R}}{R_{1N}}\right)\left(1+\frac{R_{2R}}{R_{2N}}\right)}{\left(1+\frac{R_{1R}+R_{2R}}{R_{1N}+R_{2N}}\right)} \tag{4}$$

It is apparent from (4) that R is a random variable that is nonlinearly dependent upon the random variables R_{1R} and R_{2R}. Because of this nonlinear relationship, the probability density function of R becomes unweildly making it difficult to get much insight into the random nature of R. We will now focus on linearizing the random parts of R so that the statistical properties of R can be determined. Since the random part of the resistors is assumed to be small compared to the nominal part, the term in the denominator involving the random components can be expanded in a Taylors series and truncated after first-order terms to obtain the expression

$$R \approx \frac{R_{1N}R_{2N}}{(R_{1N}+R_{2N})}\left(1+\frac{R_{1R}}{R_{1N}}\right)\left(1+\frac{R_{2R}}{R_{2N}}\right)\left(1-\frac{R_{1R}}{R_{1N}+R_{2N}}-\frac{R_{2R}}{R_{1N}+R_{2N}}\right) \tag{5}$$

If second-order terms are neglected, (5) can be rewritten as

$$R \cong \frac{R_{1N}R_{2N}}{(R_{1N}+R_{2N})}\left(1+\frac{R_{1R}}{R_{1N}}+\frac{R_{2R}}{R_{2N}}-\frac{R_{1R}}{R_{1N}+R_{2N}}-\frac{R_{2R}}{R_{1N}+R_{2N}}\right) \tag{6}$$

It can be observed from (6) that the expression for R has been linearized in terms of the random variables R_{1R} and R_{2R}. It follows that the normalized random component of the resistance can be expressed as

$$\frac{R_R}{R_N} = \frac{R_{1R}}{R_{1N}}\frac{R_{2N}}{(R_{1N}+R_{2N})} + \frac{R_{2R}}{R_{2N}}\frac{R_{1N}}{(R_{1N}+R_{2N})} \tag{7}$$

Equation (7) is now in the form of a weighted sum of uncorrelated random variables. It follows from (7) that the variance of the normalized local random component can be expressed by

$$\sigma^2_{\frac{R_R}{R_N}} = \sigma^2_{\frac{R_{1R}}{R_{1N}}}\left(\frac{R_{2N}}{R_{1N}+R_{2N}}\right)^2 + \sigma^2_{\frac{R_{2R}}{R_{2N}}}\left(\frac{R_{1N}}{R_{1N}+R_{2N}}\right)^2 \tag{8}$$

It is well known that the normalized variance of a resistor is inversely proportional to the layout area of the resistor [Hastings, A. (2000), Lane, W. and Wrixon, G. (1989), Lin, Y. and Geiger, R. (2001)]. The proportionality constant is charaterized by the process parameter $A_{\rho N}$. This proportionality can be expressed as

$$\sigma^2_{\frac{R_{iR}}{R_{iN}}} = \frac{\mathrm{A}^2_{\rho\mathrm{N}}}{A_i} \tag{9}$$

Thus, it follows from (A1), (A2) and (6) that the normalized variance can be written as

$$\sigma^2_{\frac{R_R}{R_N}} = \frac{\mathrm{A}^2_{\rho\mathrm{N}}}{A_{TOT}}\left[\frac{1}{\mathrm{u}}(v)^2 + \frac{1}{(1-\mathrm{u})}(1-v)^2\right] \tag{10}$$

This variance of the normalized resistance can be minimized by equating the partial derivatives with respect to both u and ν to zero. It follows from (7) that the partial derivative of the variance of the normalized resistance with respect of u is given by the expression

$$\frac{\partial\sigma^2_{\frac{R_R}{R_N}}}{\partial u} = \frac{\mathrm{A}^2_{\rho\mathrm{N}}}{A_{TOT}}\left[\frac{(u-v)(u+v-2uv)}{\mathrm{u}^2(1-\mathrm{u})^2}\right] \tag{11}$$

Correspondingly, the partial derivative of the variance of the normalized resistance with respect to v can be expressed as

$$\frac{\partial \sigma^2_{\frac{R_R}{R_N}}}{\partial v} = \frac{A^2_{\rho N}}{A_{TOT}}\left[\frac{2v-2u}{u(1-u)}\right] \tag{12}$$

It thus follows from (11) and (12) by setting the partial derivatives to 0 that that a minimum will be obtained if u and v satisfy the relationship

$$u = v \tag{13}$$

This result can be summarized in the following theorem.

Theorem 1:

For a fixed total area of two resistors denoted as R_1 and R_2, the variance of the random component of the normalized resistance of the parallel connection of the two resistors assumes a minimum value if and only if the ratio of the area of R_1 to the total resistor area is equal to the ratio of the resistance of the parallel combination of the two resistors to the resistance of R_1.

The locus of points in the u-v plane that provides minimum variance is a straight line as shown in Figure 2.

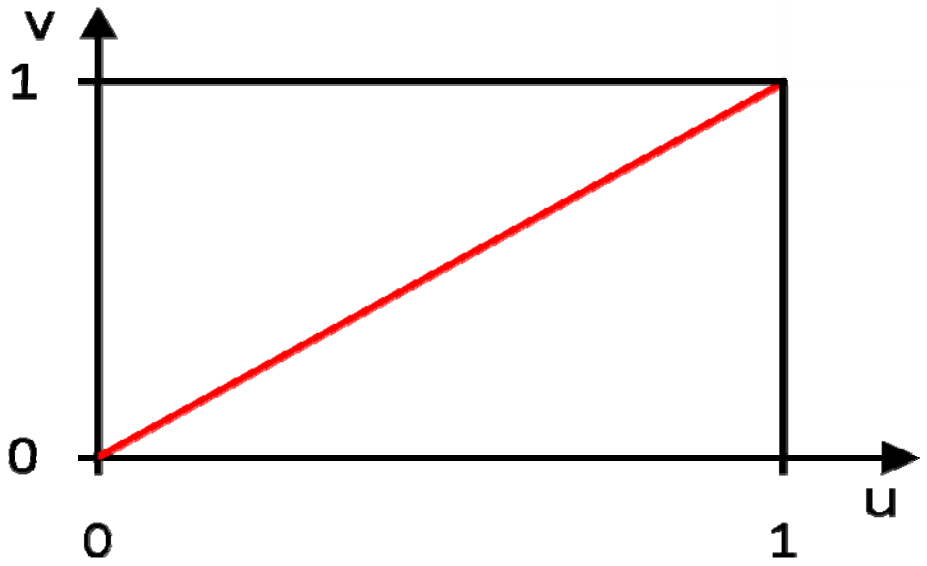

Figure 2. A locus of critical points

Substituting u = v into (10), if follows that the minimum variance or the normalized resistance is given by

$$\sigma^2_{\frac{R_R}{R_N}\Big|_{MIN}} = \frac{\mathrm{A}^2_{\rho \mathrm{N}}}{A_{TOT}} \tag{14}$$

The minimum variance is dependent upon both the process parameter and area. To establish an appreciation for the penalty incurred if non-optimal area partitioning or non-optimal resistance partitioning is used, the normalized variance is defined as

$$\sigma^2_{\frac{R_R}{R_N}\Big|_{NORM}} = \frac{\sigma^2_{\frac{R_R}{R_N}}}{\sigma^2_{\frac{R_R}{R_N}\Big|_{MIN}}} = \frac{A_{TOT}}{\mathrm{A}^2_{\rho \mathrm{N}}} \sigma^2_{\frac{R_R}{R_N}} \tag{15}$$

Deviations in the normalized variance of the normalized resistance from the optimal value for different resistance ratios and different area ratios are summarized in Table 1.

Table 1. Normalized Variance with Different Impedances And Areas

$A_1 / (A_1 + A_2)$	$R_1/ (R_1+ R_2)$				
	0.01	**0.25**	**0.5**	**0.75**	**0.99**
0.01	98.0	3.9	1.9	1.3	1
0.25	56.3	2.3	1.3	1	6.8
0.5	25.3	1.3	1	1.3	25.3
0.75	6.8	1	1.3	2.3	56.3
0.99	1	1.3	2.0	3.9	98.0

If (u,v) is on the optimal straight line, the normalized value is equal to 1 as indicated by the corresponding diagonal entries in this table. But it can be observed that if either the area partitioning or the resistance partitioning or both differ significantly from their optimal values, the penalty in variance is dramatic as can be observed by the entries in the upper left and the lower right parts of this table.

The above analysis shows that, for the same values of resistance and area of the circuit, as long as the ratio of the layout area of one resistor to the total area of the circuit is equal to the ratio of the equivalent resistance to its resistance, the variance of the equivalent random resistance is minimum. Correspondingly, if the layout area of one resistor is very big or very small and the resistance values are not sized favorably, the variance will be very large. As expected, the value selected for the total resistance is arbitrary provided the resistance partitioning and area partitioning is done in an optimal way.

2.2 The INL variance of dual ladders R String DAC

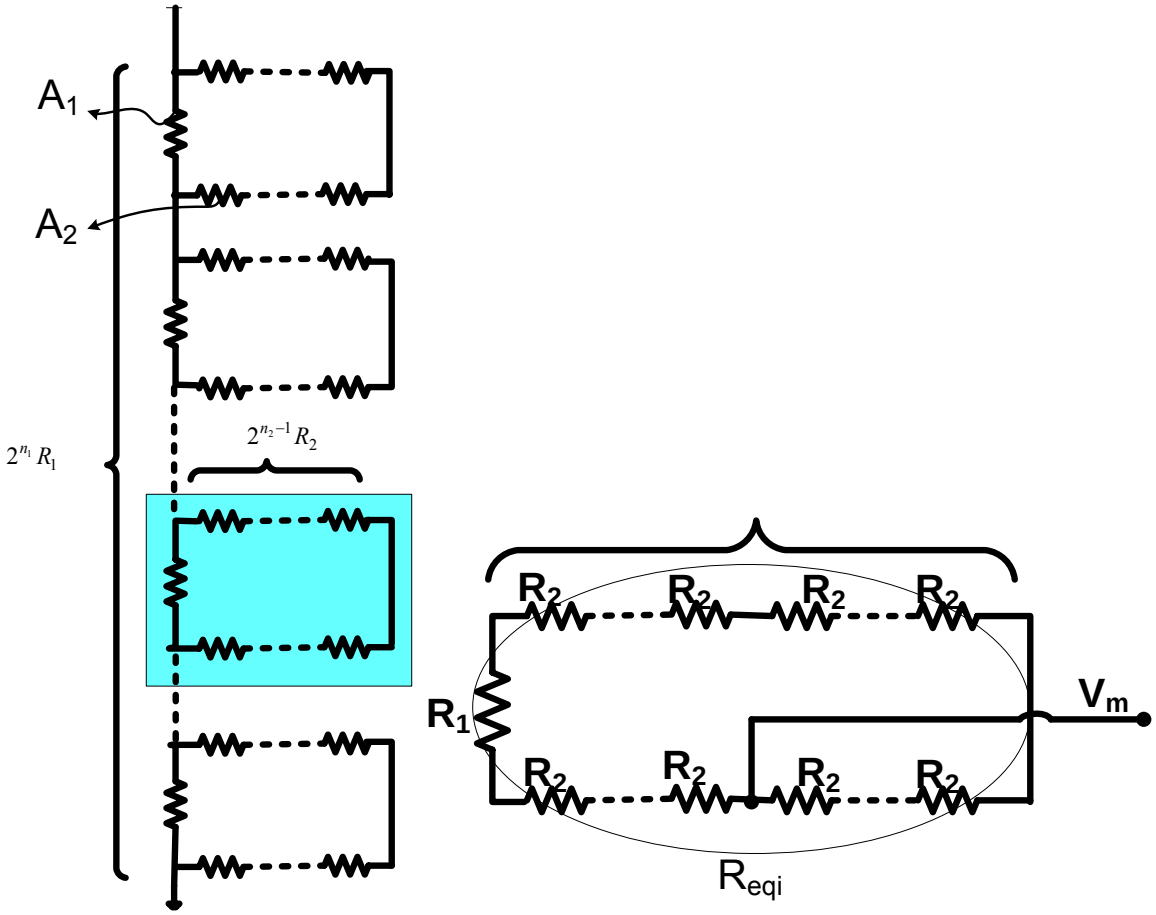

Figure 3. A Dual Resistor String Ladder

In this section, the performance of a dual –ladder resistor string DAC is characterized. Specifically, the effects of area and resistance partitioning between the coarse and fine strings on the variance of the integral nonlinearity (INL) are investigated.

The widely-used dual-string ladder structure is shown in Figure 3. The coarse ladder is comprised of 2^{n_1} coarse resistors each of resistance value R_1 and area A_1. A fine string is connected in parallel with each coarse-string resistor. Each fine string provides 2^{n_2} tap voltages as shown in Figure 3. Each resistor in the fine string ideally has a resistance of R_2

and an area of A_2. If the tap voltages are selected with switches and if this selection is done in such a way that any one of the tap voltages can be selected with a Boolean input variable, the dual-string ladder forms an n-bit DAC where $n = n_1+n_2$. For notational convenience, the switches and the Boolean input variables are not shown in Figure 3 but throughout this thesis no attempt will be made to distinguish between the dual-string ladder and the corresponding DAC that is derived from this ladder. Since emphasis will be focused exclusively on the effects of the dual-string ladder on the performance of the DAC, the switches and the Boolean logic needed to form the DAC from the dual-string ladder will be assumed to be ideal throughout this thesis.

With this understanding, the total area of the DAC is

$$A_{TOT} = 2^{n_1} A_1 + 2^{n_1}\left(2^{n_2} A_2\right) \tag{16}$$

Intergral nonlinearity (INL) error is used to measure the static accuracy of the converter. For a n-bit DAC, the INL_m of the tap voltage m ($0 \le m < 2^n$) is the difference between the voltage at the tap m and the idea voltage $m\frac{V_{REF}}{2^n}$ in LSB. The INL is the maximum of INL_m for $0 \le m < 2^n$.

The variance of the INL_m on each of 2^n tap voltages is derived and the allocation of areas and resistor values on both ladders is obtained that provides the minimum value of the maximum error in the INL profile.

2.2.1 Normalized variance of the equivalent tap resistance

As was the case for the two resistor network, it is convenient to normalize the impedances and the areas in the dual-string ladder. The normalization factors x and z are

defined to represent the ratio of the coarse ladder area to the total area of DAC and the ratio of the total equivalent resistance of the DAC to the total resistance on the coarse ladder

$$x = \left(\frac{2^{n_1} A_1}{A_{TOT}} \right) \tag{17}$$

$$z = \frac{R_{TOT}}{2^{n_1} R_1} \tag{18}$$

where A_1 is the area of a single coarse resistor and $R_{TOT} = 2^{n_1}\left(R_1 // \left(2^{n_2} R_2\right)\right)$.

The resistance in a coarse ladder tap i is defined to be the parallel combination of the coarse resistor in position i and the fine resistors paralleling this coarse resistor. Thus, the equivalent resistance in coarse ladder tap i can be expressed as

$$R_{eq,i} = \frac{R_{1i} \times \sum_{j=1}^{2^{n_2}} R_{2,ij}}{R_{1i} + \sum_{j=1}^{2^{n_2}} R_{2,ij}} \tag{19}$$

If a common centroid layout is used, the gradient component of this equivalent resistor can be ignored and resistor can be decomposed into the sum of the nominal resistance and the component due to the local random variations. It thus follows that

$$R_{eq,i}=\left(\frac{2^{n_2}R_{1N}R_{2N}}{R_{1N}+2^{n_2}R_{2N}}\right)\frac{\left(1+\frac{R_{1R,i}}{R_{1N}}\right)\left(1+\frac{\sum_{j=1}^{2^{n_2}}R_{2R,ij}}{2^{n_2}R_{2N}}\right)}{\left(1+\frac{R_{1R}+\sum_{j=1}^{2^{n_2}}R_{2R,ij}}{R_{1N}+2^{n_2}R_{2N}}\right)} \tag{20}$$

where the subscript N is used to denote the nominal part of a resistor and the subscript R is used to denote the random part of the resistor. It is apparent that the random variable R_{eqi} is itself nonlinearly dependent upon a large number of separate random variables. Following the approach used in the two resistor case discussed in the previous section, we will now linearize the random component of R_{eqi}. With this goal in mind, the denominator of (20) can first be expanded in a Taylors series. Since the random components of all random variables in (20) are small compared to their nominal componnets, after multiplying out the resultant product terms in the numerator and truncating the resultant expression after the first-order terms, we obtain:

$$R_{eq,i}\approx\left(\frac{2^{n_2}R_{1N}R_{2N}}{R_{1N}+2^{n_2}R_{2N}}\right)\left(1+\frac{R_{1R,i}}{R_{1N}}+\frac{\sum_{j=1}^{2^{n_2}}R_{2R,ij}}{2^{n_2}R_{2N}}-\frac{R_{1R,i}}{R_{1N}+2^{n_2}R_{2N}}-\frac{\sum_{j=1}^{2^{n_2}}R_{2R,ij}}{R_{1N}+2^{n_2}R_{2N}}\right) \tag{21}$$

It follows that the ratio of the equivalent resistance to the normalized equivalent resistance is

$$\frac{R_{eq,i}}{R_{eqN,i}} \approx 1+\left(\frac{R_{1R,i}}{R_{1N,i}}\right)\left(\frac{2^{n_2}R_{2N}}{R_{1N}+2^{n_2}R_{2N}}\right)+\frac{1}{2^{n_2}}\left(\frac{\sum_{j=1}^{2^{n_2}}R_{2R,ij}}{R_{2N}}\right)\left(\frac{R_{1N}}{R_{1N}+2^{n_2}R_{2N}}\right) \quad (22)$$

Since the random variables in (22) are uncorrelated, it follows that the normalized variance of the equivalent resistance in any coarse ladder tap can be expressed by

$$\sigma^2_{\frac{R_{eq}}{R_{eqN}}} = \left(\frac{2^{n_2}R_{2N}}{R_{1N}+2^{n_2}R_{2N}}\right)^2 \sigma^2_{\frac{R_{1R}}{R_{1N}}} + \left(\frac{R_{1N}}{R_{1N}+2^{n_2}R_{2N}}\right)^2 \frac{1}{(2^{n_2})^2} 2^{n_2}\left(\sigma^2_{\frac{R_{2R}}{R_{2N}}}\right) \quad (23)$$

It follows from (14), (15) that (23) can be written as

$$\sigma^2_{\frac{R_{eq}}{R_{eqN}}} = \frac{2^{n_1}A^2_{\rho N}}{A_{TOT}}\left[\left(\frac{2^{n_2}R_{2N}}{R_{1N}+2^{n_2}R_{2N}}\right)^2 \frac{A_{TOT}}{2^{n_1}A_1} + \left(\frac{R_{1N}}{R_{1N}+2^{n_2}R_{2N}}\right)^2 \frac{A_{TOT}}{A_{TOT}-2^{n_1}A_1}\right] \quad (24)$$

2.2.2 Variance of the INL

Up to this point emphasis has been focused on the statistical characterization of the resistors in the DAC. In this section emphasis will be directed to the statistical characterization of the INL. The statistical characterization of the INL of the dual-string DAC itself is very challenging since it is an order statistic of 2^n random variables. Emphasis in this section will focus on the much easier but still tedious task of characterizing the individual INL_m variables.

The output voltage at the tap

$$m = p \times 2^{n_2} + q \quad (25)$$

for $0 \le p < 2^{n_1}$ and $0 \le q < 2^{n_2}$, of the fine string ladder can be expressed as

$$V_m = \frac{V_{REF}}{\sum_{i=1}^{2^{n_1}} R_{eq,i}} \left[\sum_{i=1}^{p} R_{eq,i} + R_{eq,p+1} \left(\frac{\sum_{j=1}^{q} R_{2j}}{\sum_{j=1}^{2^{n_2}} R_{2j}} \right) \right] \tag{26}$$

Neglecting the process and gradient components of the resistors, each resistor can be decomposed into the sum of a normial resistance and the local random resistance. It thus follows from (26) that the tap voltage can be expressed as :

$$V_m = \frac{V_{REF}}{2^{n_1} R_{eqN} \left(1 + \frac{\sum_{i=1}^{2^{n_1}} R_{eqR,i}}{2^{n_1} R_{eqN}} \right)} \left[pR_{eqN} \left(1 + \frac{\sum_{j=1}^{p} R_{eqR,i}}{pR_{eqN}} \right) + R_{eqN} \left(1 + \frac{R_{eqR,p+1}}{R_{eqN}} \right) \frac{qR_{2N} \left(1 + \frac{\sum_{j=1}^{q} R_{2Rj}}{qR_{2N}} \right)}{2^{n_2} R_{2N} \left(1 + \frac{\sum_{j=1}^{2^{n_2}} R_{2Rj}}{2^{n_2} R_{2N}} \right)} \right] \tag{27}$$

where R_{2N} and R_{1N} are as defined previously and $R_{eqN}=R_{1N}//(2^{n}{}_2R_{2N})$. As was the case in the previous section, the expression for V_m is a highly nonlinear function of the random resistive variables. But, since in practical applications the random component of each resistor will be small compared to its nominal part, this nonlinear function can be linearized.

As part of the linearization, each factor of the denominators can be expanded in a Taylors series and truncated after the first-order terms to obtain:

$$V_m = \left(\frac{V_{REF}}{2^n} \right) \left[2^{n_2} p \left(1 + \frac{\sum_{i=1}^{p} R_{eqR,i}}{pR_{eqN}} \right) \left(1 - \frac{\sum_{i=1}^{2^{n1}} R_{eqR,i}}{2^{n_1} R_{eqN}} \right) + q \left(1 + \frac{R_{eqR,p+1}}{R_{eqN}} \right) \left(1 + \frac{\sum_{j=1}^{q} R_{2Rj}}{qR_{2N}} \right) \left(1 - \frac{\sum_{j=1}^{2^{n_2}} R_{2Rj}}{2^{n_2} R_{2N}} \right) \left(1 - \frac{\sum_{i=1}^{2^{n_1}} R_{eqR,i}}{2^{n_1} R_{eqN}} \right) \right] \tag{28}$$

By expanding equation (28) and neglecting higher-order terms involving the random variables, it follow that

$$V_m=\left(\frac{V_{REF}}{2^n}\right)\left[2^{n_2}p+q+2^{n_2}\frac{\sum_{i=1}^{p}R_{eqR,i}}{R_{eqN}}-2^{n_2-n_1}p\frac{\sum_{i=1}^{2^{n_1}}R_{eqR,i}}{R_{eqN}}+q\frac{R_{eqR,p+1}}{R_{eqN}}+\frac{\sum_{j=1}^{q}R_{2Rj}}{R_{2N}}-2^{-n_2}q\frac{\sum_{j=1}^{2^{n_2}}R_{2Rj}}{R_{2N}}-2^{-n_1}q\frac{\sum_{i=1}^{2^{n_1}}R_{eqR,i}}{R_{eqN}}\right] \quad (29)$$

The INL profile in LSB ($V_{LSB}=V_{REF}/2^n$) is the difference betweeen V_m and the ideal tap voltage $m\frac{V_{REF}}{2^n}$ in LSB. In the equation (29), the first two items of the sum are equal to m. Therefore, the INL_m can be written as a linear weighted sum of uncorrelated random variables as:

$$\begin{aligned}INL_m=&\left(2^{n_2}-p\times2^{n_2-n_1}-q\times2^{-n_1}\right)\left(\sum_{i=1}^{p}\frac{R_{eqR,i}}{R_{eqN}}\right)+\left(q-p\times2^{n_2-n_1}-q\times2^{-n_1}\right)\left(\frac{R_{eqR,p+1}}{R_{eqN}}\right)\\&+\left(-p\times2^{n_2-n_1}-q\times2^{-n_1}\right)\sum_{i=p+2}^{2^{n_1}}\frac{R_{eqR,i}}{R_{eqN}}+\left(1-q\times2^{-n_2}\right)\sum_{i=1}^{q}\frac{R_{2R,i}}{R_{2N}}-q\times2^{-n_2}\sum_{i=q+1}^{2^{n_2}}\frac{R_{2R,i}}{R_{2N}}\end{aligned} \quad (30)$$

Since the random variables in (30) are uncorrelated, the variance of INL_m can be expressed as:

$$\begin{aligned}\sigma^2_{INL_m}=&\sigma^2_{\frac{R_{eqR}}{R_{eqN}}}\left[\left(2^{n_2}-p\times2^{n_2-n_1}-q\times2^{-n_1}\right)^2p+\left(p\times2^{n_2-n_1}+q\times2^{-n_1}\right)^2(2^{n_1}-p-1)\right.\\&\left.+\left(q-p\times2^{n_2-n_1}-q\times2^{-n_1}\right)^2\right]+\sigma^2_{\frac{R_{2R}}{R_{2N}}}\left[q\left(1-q\times2^{-n_2}\right)^2+q^2\times2^{-2n_2}\left(2^{n_2}-q\right)\right]\end{aligned} \quad (31)$$

It follows from (16) and (17) that $\sigma^2_{\frac{R_{2R}}{R_{2N}}}$ can be expressed as:

$$\sigma^2_{\frac{R_{2R}}{R_{2N}}}=\frac{A^2_{\rho N}}{A_2}=\frac{A^2_{\rho N}}{A_{TOT}}\times\frac{2^n}{(1-x)} \quad (32)$$

From (24),(31), and (32), it follows that

$$\sigma^2_{INL_m} = \frac{2^{n_1}A^2_{\rho N}}{A_{TOT}}\left[\frac{z^2}{x}+\frac{(1-z)^2}{(1-x)}\right]\left[\left(2^{n_2}-p\times 2^{n_2-n_1}-q\times 2^{-n_1}\right)^2 p+\left(p\times 2^{n_2-n_1}+q\times 2^{-n_1}\right)^2 (2^{n_1}-p-1)\right. \quad (33)$$
$$\left.+\left(q-p\times 2^{n_2-n_1}-q\times 2^{-n_1}\right)^2\right]+\frac{A^2_{\rho N}}{A_{TOT}}\frac{2^n}{(1-x)}\left[q\left(1-q\times 2^{-n_2}\right)^2+q^2\times 2^{-2n_2}\left(2^{n_2}-q\right)\right]$$

Relative size and impedance information is carried in the two variables x and z. For convenience, the normalized variance of INL_m is defined as:

$$\sigma^2_{NORM}(INL_m) = \frac{A_{TOT}}{2^{2n-2}A^2_{\rho N}}\sigma^2_{INL_m} \quad (34)$$

The function (33) can be minimized by differetiating (33) with respect to x and z and setting the patial derivative to zero. Thus differentiating $\sigma^2_{NORM}(INL_m)$ with respect to z, we obtain

$$\frac{\partial\sigma^2_{INLm}}{\partial z}(x,z)=\frac{A^2_{\rho N}}{A_{TOT}}2^{n1}\left[\left(2^{n_2}-p\times 2^{n_2-n_1}-q\times 2^{-n_1}\right)^2 p+\left(q-p\times 2^{n_2-n_1}-q\times 2^{-n_1}\right)^2+\left(p\times 2^{n_2-n_1}+q\times 2^{-n_1}\right)^2(2^{n_1}-p-1)\right]\left[\frac{2(z-x)}{x(1-x)}\right] \quad (35)$$

Setting $\frac{\partial\sigma^2_{INLm}}{\partial z}(x,z)=0$, it follows that x = z. Notice this solution is independent of m and independent of $A^2_{\rho N}/A_{TOT}$. Therefore, for a given x, the normalized variance of the local random component in the dual-string DAC is minimum if the ratio of the total impedance to the coarse ladder impedance is equal to the ratio of the layout coarse area to the total area of the circuit. This is summarized in the following theorem.

Theorem 2:

For a given x and for all m, the variance of INL_m for a dual string DAC is minimized when z = x where $x = A_C/A_{TOT}$ and $z = R_{TOT}/R_C$.

Although for a given value of x, a local minimum of the variance of INL_m in the variable z can be obtained, there is no local minimum in the open unit square in the (x,z)

plane. But, it can also be shown that if x = z, then the variance decreases with x. And, in the latter case, the decrease in variance as x approaches 0 is very small. These observations can be summarized in the following theorems.

Theorem 3:

For all m, the variance of INL_m for a dual string DAC does not assume a local minimum in $\{ (x,z)| 0 < x < 1, 0 < z < 1 \}$, where $x = A_C/A_{TOT}$ and $z = R_{TOT}/R_C$.

Theorem 4:

For all m, the variance of INL_m for a dual string DAC decreases monotonically as x approaches 0 on the x = z locus where $x = A_C/A_{TOT}$ and $z = R_{TOT}/R_C$.

Theorem 5:

The derivatives of the variance of INL_{MAX} for a dual string DAC along the x=z line in the x-z plane is small for $0 < z < \varepsilon$, where $0 < \varepsilon \ll 1$ where $x = A_C/A_{TOT}$ and $z = R_{TOT}/R_C$.

Although Theorem 5 states that the variance changes very slowly along the x=z line in the x-z plane, it should be emphasized that this Theorem does not state that the variance changes very slowly near the origin of the x-z plane and, in fact, it can change significantly near the orgin at points that are not on the x=z line.

The open unit square in the x-z plane is shown in Figure 4 along with the x = z line which represents the optimal value of z for a given value of x. It thus follows that if a design has paramaters (x,z) that are close to the x = z line, the variance of INL_{MAX} should be near optimal. A tight lower bound on the variance occurs on the boundary of the unit square at the point (0,0). As Theorem 5 indicates, when operating on the x = z line near the orgin, the

variance of INL_{MAX} should be near the tight lower bound. It will be shown in Chapter 3 that when operating with paramaters that deviate significantly from the x = z line, the variance of the INL_{MAX} may be significantly larger than optimal.

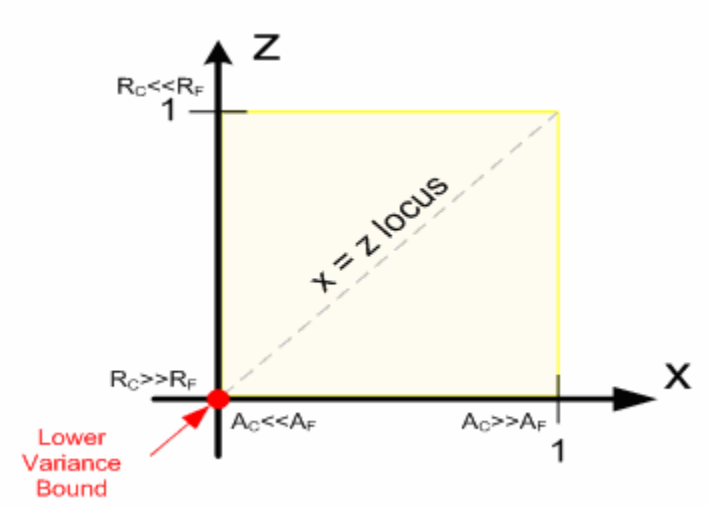

Figure 4. Region of Operation for Dual-String DAC in the x - z plane

As an example, the minimum INL as a function of z, for a 10-bit dual ladder string DAC with 4 bits allocated to the coarse string is ploted in Figure 5 for different values of x. From this plot it is apparent that the local minimum is rather shallow for x around 0.5 but becomes much steeper for extreme values of x approaching 0 or 1. It is apparent that if a non-optimal allocation of area or impedance is used, the penalty in the variance, and correspondingly the yield, can be quite large. It is also shown the smaller values of x are, the smaller variance is obtained although the differences in the minimum INL do not change dramatically as x is changed. If there is no coarse ladder, which would correspond to x=z=0, σ(INL) will assume its minimum value. But we can not eliminate the coarse ladder because without the coarse ladder, the gradient effects would need to be managed by the fine string

resistors and common centroid layouts that cancel the gradient effects would be difficult to realize if the resolution of the DAC was very large.

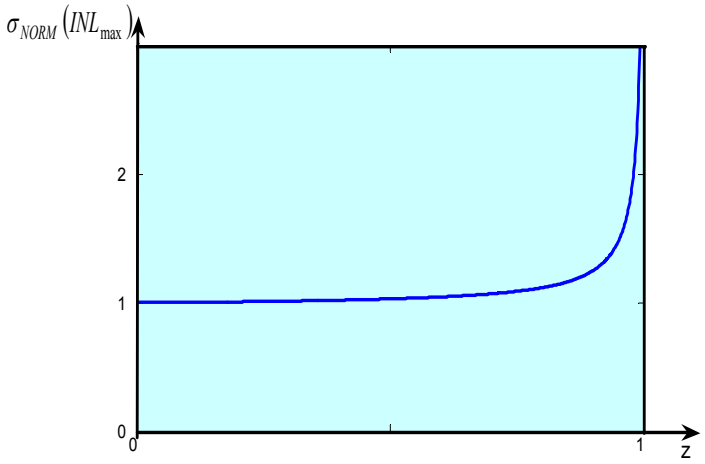

Figure 5. The minimum of $\sigma_{NORM}(INL_{max})$ for a given z

A plot of the normalized variance for different values of x along the x=z locus is shown in Figure 5. From Figure 5 it can be sent that the minimum normalized standard deviation is 512 but the minimum is very shallow on the x = z locus with an increase above the minimum of only 3% for x = z = 0.5 and of only 48% even when x=z=0.95. Thus, the benefits of having extreme values of x and z provided x = z are not substantial. But, for a given z, when x deviates from z, the penalty in the variance and correspondingly the yield is significant. This can be seen in Figure 6 where the maximum variance is plotted versus x for z fixed at 0.5.

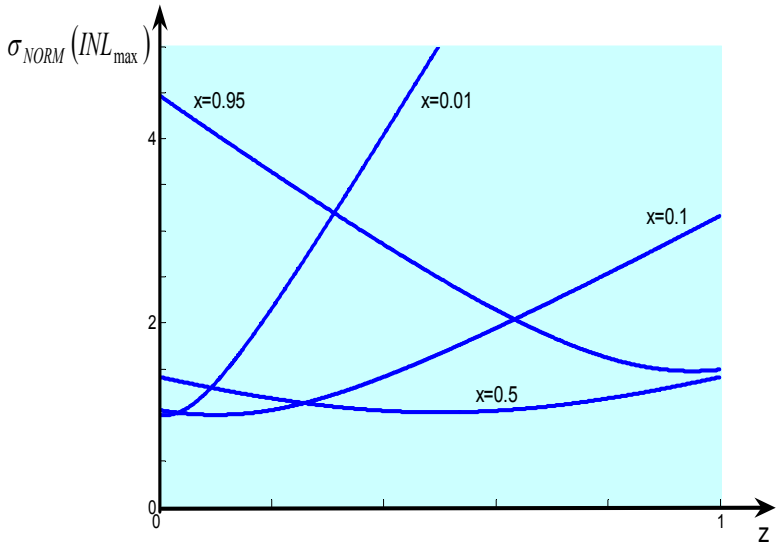

Figure 6. $\sigma_{NORM}(INL_{max})$ w.r.t. x

2.3 The INL variance of Interpolation DAC with buffer

In this section, a different dual-ladder DAC is considered. This structure uses buffers to connect the fine string to the coarse ladder thus dramatically reducing the total number of resistors needed by the fine string. This approach also eliminates the loading of the coarse string by the fine string at dc. This structure is shown in Figure 7. As in the previous section, emphasis will be placed on characterizing and minimizing the variance of the INL_m in this section.

For the buffered structure of Figure 7, the coarse ladder consists of 2^{n_1} coarse resistors of resistance value R_1 and area A_1. The fine string is comprised of 2^{n_2} resistors, each with a resistance of R_2 and an area A_2. For each connection of the intropolator to the coarse string, the interpolator provides to the output 2^{n_2} tap voltages.

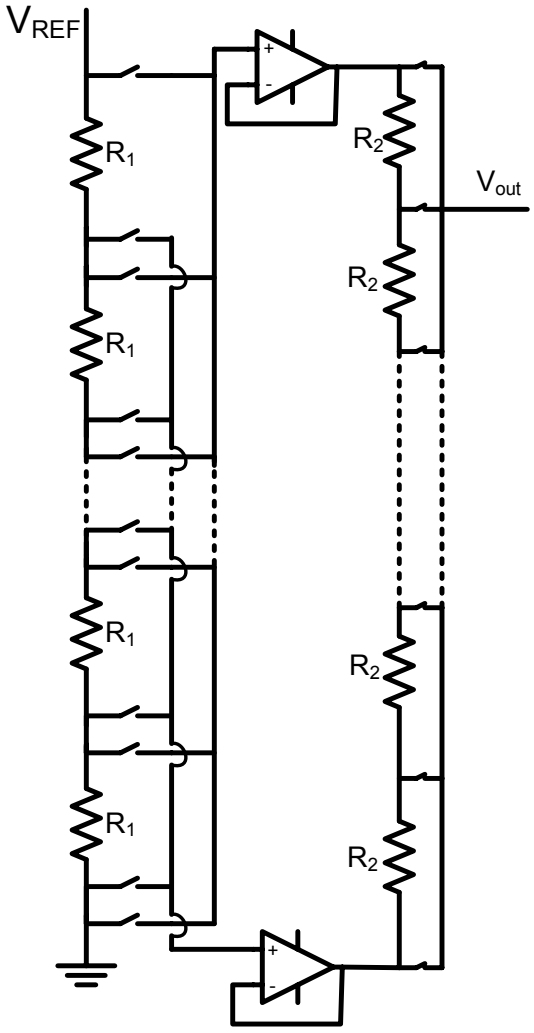

Figure 7. The Interpolation DAC with buffers

As for the dual ladder structure in the previous section, the total number of tap voltages is 2^n, where $n=n_1+n_2$. The variance of the INL_m on each of 2^n tap voltages will be derived and the allocation of area and resistance on both ladders to obtain the minimum value of the maximum error in the INL profile will be obtained.

Let x be the ratio of the coarse ladder area to the total area of DAC,

$$x = \left(\frac{2^{n_1} A_1}{A_{TOT}} \right) \tag{36}$$

where $A_{TOT} = 2^{n1}A_1 + 2^{n2}A_2$. The output voltage at the tap $m = p \times 2^{n_2} + q$, $0 \le p < 2^{n_1}$ and $0 \le q < 2^{n2}$, of the fine string ladder is expressed as:

$$V_m = \frac{V_{REF}}{\sum_{i=1}^{2^{n1}} R_{1,i}} \left[\sum_{i=1}^{p} R_{1,i} + R_{1,p+1} \left(\frac{\sum_{j=1}^{q} R_{2j}}{\sum_{j=1}^{2^{n2}} R_{2j}} \right) \right] \tag{37}$$

Neglecting the process and gradient component of the resistor, it follows that

$$V_m = \frac{V_{REF}}{2^{n_1} R_{1N} \left(1 + \frac{\sum_{1}^{2^{n1}} R_{1R,i}}{2^{n_1} R_{1N}} \right)} \left[pR_{1N} \left(1 + \frac{\sum_{1}^{p} R_{1R,i}}{pR_{1N}} \right) + R_{1N} \left(1 + \frac{R_{1R,p+1}}{R_{1N}} \right) \frac{qR_{2N} \left(1 + \frac{\sum_{1}^{q} R_{2Rj}}{qR_{2N}} \right)}{2^{n_2} R_{2N} \left(1 + \frac{\sum_{1}^{2^{n2}} R_{2Rj}}{2^{n_2} R_{2N}} \right)} \right] \tag{38}$$

where the subscripts R and N refer to the random part and the nominal part of the resistances. This function is highly nonlinear in the random components of the resistances but since the random components are assumed small compared to the nominal part of the resistors, this function can be linearized.

To linearize this function, first each factor of the denominator can be expanded in Taylors series and truncated after the first-order terms to obtain:

$$V_m = \left(\frac{V_{REF}}{2^n} \right) \left[2^{n_2} p \left(1 + \frac{\sum_{i=1}^{p} R_{1R,i}}{pR_{1N}} \right) \left(1 - \frac{\sum_{i=1}^{2^{n1}} R_{1R,i}}{2^{n_1} R_{1N}} \right) + q \left(1 + \frac{R_{1R,p+1}}{R_{1N}} \right) \left(1 + \frac{\sum_{j=1}^{q} R_{2Rj}}{qR_{2N}} \right) \left(1 - \frac{\sum_{j=1}^{2^{n2}} R_{2Rj}}{2^{n_2} R_{2N}} \right) \left(1 - \frac{\sum_{i=1}^{2^{n1}} R_{1R,i}}{2^{n_1} R_{1N}} \right) \right] \tag{39}$$

Expanding equation (39) and neglecting the higher-order terms, we obtain the following equation:

$$V_m = \left(\frac{V_{REF}}{2^n}\right)\left[2^{n_2}\,p + q + 2^{n_2}\frac{\sum_{i=1}^{p} R_{1R,i}}{R_{1N}} - 2^{n_2-n_1}\,p\frac{\sum_{i=1}^{2^{n1}} R_{1R,i}}{R_{1N}} + q\frac{R_{1R,p+1}}{R_{1N}} + \frac{\sum_{j=1}^{q} R_{2Rj}}{R_{2N}} - 2^{-n_2}\,q\frac{\sum_{j=1}^{2^{n2}} R_{2Rj}}{R_{2N}} - 2^{-n_1}\,q\frac{\sum_{i=1}^{2^{n1}} R_{1R,i}}{R_{1N}}\right] \quad (40)$$

The INL profile in LSB ($V_{LSB} = V_{REF}/2^n$) is the difference betweeen V_m and the ideal tap voltage $mV_{REF}/2^n$ in LSB. In equation (40), two first items in the brackets are equal to the order of the tap m. Thus, the INL_m can be written as:

$$\mathrm{INL_m} = \left(2^{n_2} - \mathrm{p}\times 2^{n_2-n_1} - \mathrm{q}\times 2^{-n_1}\right)\left(\sum_{i=1}^{p}\frac{R_{1R,i}}{R_{1N}}\right) + \left(\mathrm{q} - \mathrm{p}\times 2^{n_2-n_1} - \mathrm{q}\times 2^{-n_1}\right)\left(\frac{R_{1R,p+1}}{R_{1N}}\right) \quad (41)$$

$$+\left(-\mathrm{p}\times 2^{n_2-n_1} - \mathrm{q}\times 2^{-n_1}\right)\sum_{i=p+2}^{2^{n_1}}\frac{R_{1R,i}}{R_{1N}} + \left(1 - \mathrm{q}\times 2^{-n_2}\right)\sum_{i=1}^{q}\frac{R_{2R,i}}{R_{2N}} - \mathrm{q}\times 2^{-n_2}\sum_{i=q+1}^{2^{n_2}}\frac{R_{2R,i}}{R_{2N}}$$

Equation (41) is now the weighted sum of uncorrelated random variables and thus, the variance of INL_m can be expressed as:

$$\sigma^2_{INL_m} = \sigma^2_{\frac{R_{1R}}{R_{1N}}}\left[\left(2^{n_2} - p\times 2^{n_2-n_1} - q\times 2^{-n_1}\right)^2 p + \left(p\times 2^{n_2-n_1} + q\times 2^{-n_1}\right)^2 (2^{n_1} - p - 1)\right.$$
$$\left.+\left(q - p\times 2^{n_2-n_1} - q\times 2^{-n_1}\right)^2\right] + \sigma^2_{\frac{R_{2R}}{R_{2N}}}\left[q\left(1 - q\times 2^{-n_2}\right)^2 + q^2\times 2^{-2n_2}\left(2^{n_2} - q\right)\right] \quad (42)$$

By subsituting $\sigma^2_{\frac{R_{1R}}{R_{1N}}} = \frac{A^2_{\rho N}}{A_1}$, $\sigma^2_{\frac{R_{2R}}{R_{2N}}} = \frac{A^2_{\rho N}}{A_2} = A^2_{\rho N}\frac{2^{n_2}}{A_T - 2^{n_1}A_1}$ and $x = \left(\frac{2^{n_1}A_1}{A_{TOT}}\right)$, (42) can be written as

$$\sigma^2_{INL_m} = \frac{A^2_{\rho N}}{A_{TOT}}\left\{\frac{2^{n_1}}{x}\left[\left(2^{n_2} - p\times 2^{n_2-n_1} - q\times 2^{-n_1}\right)^2 p + \left(p\times 2^{n_2-n_1} + q\times 2^{-n_1}\right)^2 (2^{n_1} - p - 1)\right.\right.$$
$$\left.\left.+\left(q - p\times 2^{n_2-n_1} - q\times 2^{-n_1}\right)^2\right] + \frac{2^{n_2}}{1-x}\left[q\left(1 - q\times 2^{-n_2}\right)^2 + q^2\times 2^{-2n_2}\left(2^{n_2} - q\right)\right]\right\} \quad (43)$$

This variance is dependent upon the total area, A_{TOT}, and the process parameter $A_{\rho N}$. By normalizing the variance by $A^2_{\rho N}/A_{TOT}$, the effects of x and m on the INL_m can be practically depicted. With this normalization, (43) simplifies to

$$\sigma^2_{NORM}(INL_m)=\frac{2^{n_1}}{x}\left[\left(2^{n_2}-p\times 2^{n_2-n_1}-q\times 2^{-n_1}\right)^2 p+\left(p\times 2^{n_2-n_1}+q\times 2^{-n_1}\right)^2(2^{n_1}-p-1)\right.$$
$$\left.+\left(q-p\times 2^{n_2-n_1}-q\times 2^{-n_1}\right)^2\right]+\frac{2^{n_2}}{1-x}\left[q\left(1-q\times 2^{-n_2}\right)^2+q^2\times 2^{-2n_2}\left(2^{n_2}-q\right)\right] \quad (44)$$

To find the optimum of area allocation, the derivative of (44) with respect to x is taken and set to zero. Thus, differentiating $\sigma^2_{NORM}(INL_m)$ with respect to x, we obtain:

$$\frac{\partial\sigma^2_{NORM}(INL_m)}{\partial x}=\frac{-2^{n_1}\left[\left(2^{n_2}-p\times 2^{n_2-n_1}-q\times 2^{-n_1}\right)^2 p+\left(p\times 2^{n_2-n_1}+q\times 2^{-n_1}\right)^2(2^{n_1}-p-1)\right.}{x^2}$$
$$\left.\frac{+\left(q-p\times 2^{n_2-n_1}-q\times 2^{-n_1}\right)^2}{x^2}\right]+\frac{2^{n_2}\left[q\left(1-q\times 2^{-n_2}\right)^2+q^2\times 2^{-2n_2}\left(2^{n_2}-q\right)\right]}{(1-x)^2} \quad (45)$$

Setting $\frac{\partial\sigma^2_{NORM}(INL_m)}{\partial x}=0$, it follows that

$$x=\frac{b_1\pm\sqrt{b_1 b_2}}{b_1-b_2} \quad (46)$$

for

$$b_1=2^{n_1}\left[\left(2^{n_2}-p\times 2^{n_2-n_1}-q\times 2^{-n_1}\right)^2 p+\left(q-p\times 2^{n_2-n_1}-q\times 2^{-n_1}\right)^2\right.$$
$$\left.+\left(p\times 2^{n_2-n_1}+q\times 2^{-n_1}\right)^2(2^{n_1}-p-1)\right] \quad (47)$$

$$b_2=2^{n_2}\left[q\left(1-q\times 2^{-n_2}\right)^2+q^2\times 2^{-2n_2}\left(2^{n_2}-q\right)\right] \quad (48)$$

2.4 The INL variance of Interpolation Resistor String DAC with buffer resistors

A third variant of the dual string DAC is shown in Figure 8. Conventional wisdom teaches that this structure eliminates the need for the buffers of the previous structure and uses extra "replacement" resistors to prevent having the interpolating fine-string resistor load a coarse string resistor. Although the nominal value of the "replacement" resistor is ideally equal to that of the fine interpolation string, the area can usually be made much smaller. In this section, the DAC of Figure 8 the variance of INL of this DAC will be characterized.

The coarse ladder is consists of 2^{n_1} coarse resistors of resistance value R_1 and area A_1. A fine string is connected in parallel with only one coarse resistor at any time and determines 2^{n_2} tap voltages. Each replacement resistor R_3, having a nominal resistance of $2^{n2}R_2$ and an area of A_3, is connected in parallel with a resistor of the coarse ladder R_1 if the fine string interpolator is not connected to a given coarse ladder resistor. Thus, there is always 2^{n1}-1 replacement resistors along with the fine-string interpolation circuit connected in parallel with each of the coarse string resistors.

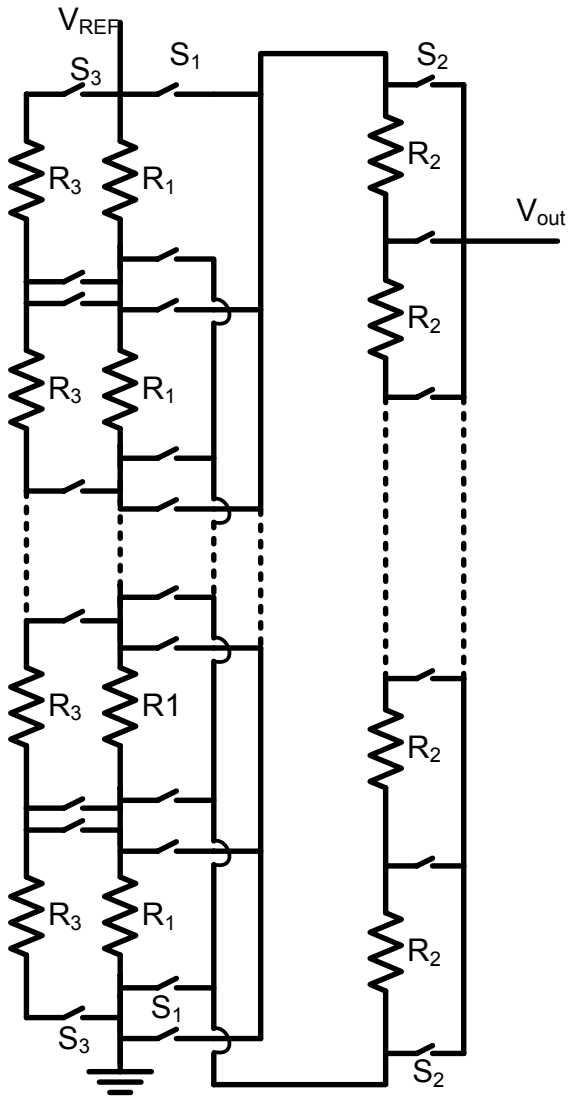

Figure 8. Dual Resistor String with Buffer Resistors

As was the case for the two previous dual-string resistor arrays, the total number of tap voltages is 2^n, where $n=n_1+n_2$. The variance of the INL_m on each of 2^n tap voltages will be derived and the allocation of areas and resistance values on both ladders will be given that provides a minimum value of the maximum error in the INL profile.

2.4.1 The normalized variance of resistances

In contrast to the previous two circuits where the switch impedance did not affect the static performance of the DAC, in this structure, the switch impedance is in series with either the replacement resistor or the fine-string interpolation resistor and, as such, contributes to the resistances in the ladder. To keep the analysis manageable, it will be assumed that the switches are all ideal and have 0Ω on impedance.

For convenience, define $R_{eq2} = R_1 // (2^{n2}R_2)$ and $R_{eq3} = R_1 // R_3$. Since ideally $R_3 = 2^{n2}R_2$, it follows that $R_{eq2} = R_{eq3}$. Thus, the nominal value of these resistors are equal to each other, $R_{eq2N} = R_{eq3N} = R_{eqN}$. As in the Section 2.2, from (24), the normalized variance of the equivalent resistance R_{eq2} is given by the expression

$$\sigma^2_{\frac{R_{eq2}}{R_{eqN}}} = \left(\frac{R_{eqN}}{R_{1N}}\right)^2 \frac{A^2_{\rho N}}{A_1} + \left(\frac{R_{eqN}}{2^{n_2} R_{2N}}\right)^2 \frac{A^2_{\rho N}}{2^{n_2} A_2} \tag{49}$$

Similarly, the normalized variance of the equivalent resistance R_{eq3} is

$$\sigma^2_{\frac{R_{eq3R}}{R_{eqN}}} = \left(\frac{R_{eqN}}{R_{1N}}\right)^2 \frac{A^2_{\rho N}}{A_1} + \left(\frac{R_{eqN}}{R_{3N}}\right)^2 \frac{A^2_{\rho N}}{A_3} \tag{50}$$

2.4.2 The variance of INL

Define z to be the ratio

$$z = \frac{R_{TOT}}{2^{n_1} R_1} \tag{51}$$

and aA_k, k = 1, 2, 3, to be the total area of the coarse string, the fine string, the replacement resistors R_3, over the total resistor area:

$$a_1 = \frac{2^{n_1} A_1}{A_{TOT}} \tag{52}$$

$$a_2 = \frac{2^{n_2} A_2}{A_{TOT}} \tag{53}$$

$$a_3 = \frac{2^{n_1} A_3}{A_{TOT}} \tag{54}$$

The output voltage at the tap $m = p \times 2^{n_2} + q$, $0 \le p \le 2^{n_1} - 1$ and $0 \le q \le 2^{n2} - 1$, of the fine string ladder for the case p > 0; q > 0 can be expressed as

$$V_m = \frac{V_{REF}}{\sum_{i=1, i \neq p+1}^{2^{n_1}} R_{eq1,i} + R_{eq2,p+1}} \left[\sum_{i=1}^{p} R_{eq1,i} + R_{eq2,p+1} \left(\frac{\sum_{j=1}^{q} R_{2j}}{\sum_{j=1}^{2^{n_2}} R_{2j}} \right) \right] \tag{55}$$

Neglecting the process and gradient components of the resistor, it follows that

$$V_m = \frac{V_{REF}}{\left[2^{n_1} R_{eqN}\right] \left(1 + \frac{\sum_{i=1}^{p} R_{eq1R,i} + \sum_{i=p+2}^{2^{n_1}} R_{eq1R,i} + R_{eq2R,p+1}}{2^{n_1} R_{eqN}} \right)} \times$$

$$\left[pR_{eqN} \left(1 + \frac{\sum_{1}^{p} R_{eq1R,i}}{pR_{eqN}} \right) + R_{eqN} \left(1 + \frac{R_{eq2R,p+1}}{R_{eqN}} \right) \frac{qR_{2N} \left(1 + \frac{\sum_{j=1}^{q} R_{2Rj}}{qR_{2N}} \right)}{2^{n_2} R_{2N} \left(1 + \frac{\sum_{j=1}^{2^{n_2}} R_{2Rj}}{2^{n_2} R_{2N}} \right)} \right] \tag{56}$$

where the subscripts R and N denote the random part and the nominal part of the corresponding random resistance value. As in the previous sections, V_m is highly nonlinear in the random variables but since the random part of the resistances is assumed to be small

compared to the nominal part, this equation can be linearized. As the first step in the linearization process, each factor of the denominator will be expanded in a Taylors series truncated after the first-order terms to obtain:

$$V_m = \left(\frac{V_{REF}}{2^n}\right)\left[2^{n_2}p\left(1+\frac{\sum_{i=1}^{p} R_{eq1R,i}}{pR_{eqN}}\right)\left(1-\frac{\sum_{i=1,i\neq p+1}^{2^{n_1}} R_{eq1R,i}}{2^{n_1}R_{eqN}}-\frac{R_{eq2R,p+1}}{2^{n_1}R_{eqN}}\right)\right. \quad (57)$$

$$\left.+q\left(1+\frac{R_{eq2R,p+1}}{R_{eqN}}\right)\left(1+\frac{\sum_{j=1}^{q} R_{2Rj}}{qR_{2N}}\right)\left(1-\frac{\sum_{j=1}^{2^{n_2}} R_{2Rj}}{2^{n_2}R_{2N}}\right)\left(1-\frac{\sum_{i=1,i\neq p+1}^{2^{n_1}} R_{eq1R,i}}{2^{n_1}R_{eqN}}-\frac{R_{eq2R,p+1}}{2^{n_1}R_{eqN}}\right)\right]$$

Expanding equation (52) and neglecting second-order and higher terms in the random variables, we obtain the following expression:

$$V_m = \left(\frac{V_{REF}}{2^n}\right)\left[2^{n_2}p+2^{n_2}\frac{\sum_{i=1}^{p} R_{eq1R,i}}{R_{eqN}}-2^{n_2-n_1}p\frac{\sum_{i=1,i\neq p+1}^{2^{n_1}} R_{eq1R,i}}{R_{eqN}}-2^{n_2-n_1}p\frac{R_{eq2R}}{R_{eqN}}+q\right. \quad (58)$$

$$\left.+q\frac{R_{eq2R,p+1}}{R_{eqN}}+\frac{\sum_{j=1}^{q} R_{2Rj}}{R_{2N}}-2^{-n_2}q\frac{\sum_{j=1}^{2^{n_2}} R_{2Rj}}{R_{2N}}-2^{-n_1}q\frac{\sum_{i=1,i\neq p+1}^{2^{n_1}} R_{eq1R,i}}{R_{eqN}}-2^{-n_1}q\frac{R_{eq2R,p+1}}{R_{eqN}}\right]$$

This expression is now in the form of a weighted sum of uncorrelated random variables.

The INL profile in LSB ($V_{LSB} = V_{REF}/2^n$)is the difference betweeen V_m and the ideal tap voltage [$m(V_{REF}/2^n)$] in LSB. The first two terms in the brackets of equation (53) are equal to the tap number m. Thus, the $INL_m = V_m - mV_{REF}/2^n$ can be written as:

$$\mathrm{INL_m} = 2^{n_2}\frac{\sum_{i=1}^{p} R_{eq1R,i}}{R_{eqN}} - 2^{n_2-n_1}p\frac{\sum_{i=1,i\neq p+1}^{2^{n_1}} R_{eq1R,i}}{R_{eqN}} - 2^{n_2-n_1}p\frac{R_{eq2R}}{R_{eqN}} + q\frac{R_{eq2R,p+1}}{R_{eqN}} \quad (59)$$
$$+\frac{\sum_{j=1}^{q} R_{2Rj}}{R_{2N}} - 2^{-n_2}q\frac{\sum_{j=1}^{2^{n_2}} R_{2Rj}}{R_{2N}} - 2^{-n_1}q\frac{\sum_{i=1,i\neq p+1}^{2^{n_1}} R_{eq1R,i}}{R_{eqN}} - 2^{-n_1}q\frac{R_{eq2R,p+1}}{R_{eqN}}$$

Thus, the variance of $\mathrm{INL_m}$ can be expressed as:

$$\sigma^2_{INL_m} = \sigma^2_{\frac{R_{eq1R}}{R_{eq1N}}}\left[\left(2^{n_2} - p\times 2^{n_2-n_1} - q\times 2^{-n_1}\right)^2 p + \left(p\times 2^{n_2-n_1} + q\times 2^{-n_1}\right)^2 (2^{n_1} - p - 1)\right]$$
$$+\sigma^2_{\frac{R_{eq2R}}{R_{eq2N}}}\left[\left(q - p\times 2^{n_2-n_1} - q\times 2^{-n_1}\right)^2\right] + \sigma^2_{\frac{R_{2R}}{R_{2N}}}\left[q\left(1 - q\times 2^{-n_2}\right)^2 + q^2\times 2^{-2n_2}\left(2^{n_2} - q\right)\right] \quad (60)$$

Subsituting

$$\sigma^2_{\frac{R_{eq2R}}{R_{eq2N}}} = \left(\frac{R_{eqN}}{R_{1N}}\right)^2\frac{A^2_{\rho N}}{A_1} + \left(\frac{R_{eqN}}{2^{n_2}R_{2N}}\right)^2\frac{A^2_{\rho N}}{2^{n_2}A_2}, \quad (61)$$

$$\sigma^2_{\frac{R_{eq1R}}{R_{eq1N}}} = \left(\frac{R_{eqN}}{R_{1N}}\right)^2\frac{A^2_{\rho N}}{A_1} + \left(\frac{R_{eqN}}{R_{3N}}\right)^2\frac{A^2_{\rho N}}{A_3} \quad (62)$$

$$\sigma^2_{\frac{R_{2R}}{R_{2N}}} = \frac{A^2_{\rho N}}{A_2} \quad (63)$$

and rearranging the order of terms in (55), we get the following equation:

$$\sigma^2_{INL_m} = \frac{A^2_{\rho N}}{A_1}\left(\frac{R_{eq1N}}{R_{1N}}\right)^2\left[\left(2^{n_2} - p\times 2^{n_2-n_1} - q\times 2^{-n_1}\right)^2 p + \left(p\times 2^{n_2-n_1} + q\times 2^{-n_1}\right)^2 (2^{n_1} - p - 1)\right.$$
$$\left. + \left(q - p\times 2^{n_2-n_1} - q\times 2^{-n_1}\right)^2\right] + \left[\frac{A^2_{\rho N}}{2^{n_2} A_2}\right]\left\{2^{n_2}\left[q\left(1 - q\times 2^{-n_2}\right)^2 + q^2\times 2^{-2n_2}\left(2^{n_2} - q\right)\right]\right.$$
$$\left. + \left(\frac{R_{eqN}}{2^{n_2} R_{2N}}\right)^2\left[\left(q - p\times 2^{n_2-n_1} - q\times 2^{-n_1}\right)^2\right]\right\} \quad (64)$$
$$+ \frac{A^2_{\rho N}}{A_3}\left(\frac{R_{eqN}}{R_{3N}}\right)^2\left[\left(2^{n_2} - p\times 2^{n_2-n_1} - q\times 2^{-n_1}\right)^2 p + \left(p\times 2^{n_2-n_1} + q\times 2^{-n_1}\right)^2 (2^{n_1} - p - 1)\right]$$

For notational convenience, define M_1, M_2 ,M_3, and M_4 by the expressions

$$M_1 = \left[\left(2^{n_2} - p\times 2^{n_2-n_1} - q\times 2^{-n_1}\right)^2 p + \left(p\times 2^{n_2-n_1} + q\times 2^{-n_1}\right)^2 (2^{n_1} - p - 1) + \left(q - p\times 2^{n_2-n_1} - q\times 2^{-n_1}\right)^2\right] \quad (65)$$

$$M_2 = \left[\left(2^{n_2} - p\times 2^{n_2-n_1} - q\times 2^{-n_1}\right)^2 p + \left(p\times 2^{n_2-n_1} + q\times 2^{-n_1}\right)^2 (2^{n_1} - p - 1)\right] \quad (66)$$

$$M_3 = \left\{\left[\left(q - p\times 2^{n_2-n_1} - q\times 2^{-n_1}\right)^2\right]\right\} \quad (67)$$

$$M_4 = \left\{2^{n_2}\left[q\left(1 - q\times 2^{-n_2}\right)^2 + q^2\times 2^{-2n_2}\left(2^{n_2} - q\right)\right]\right\} \quad (68)$$

The paramaters M_1..M_4 are dependent upon the index number but independent of model parameters, resistance values, and area.

Then (59) can be written as:

$$\sigma^2_{INL_m} = \frac{A^2_{\rho N}}{A_{TOT}}\left[2^{n_1}\frac{z^2}{a_1}M_1 + 2^{n_1}\frac{(1-z)^2}{a_3}M_2 + \frac{1}{a_2}M_4 + \frac{(1-z)^2}{a_2}M_3\right] \quad (69)$$

CHAPTER 3. SIMULATION RESULTS

In the previous chapter, analytical formulations were presented that characterizes the statistical performance for three different types of dual – ladder DACs. These parametric formulations provide the INL_m at each DAC output code and are strongly a function of the number of bits of resolution in the coarse string, the number of bits of resolution in the fine string, as well as the impedance and area allocations between the coarse and find string resistors. As such, it is challenging to obtain a practical understanding of the benefits and limitations of various area and impedance allocation schemes. In this chapter, computer simulations are presented that give insight into the benefits obtained by optimally allocating impedances and area between the coarse and fine resistor strings.

3.1 Simulation results of dual-ladder R String

In this section the performance of the dual-ladder R String of Figure 3 will be investigated. Mathematically, the INL performance of this structure is characterized by equation (33).

3.1.1 10-bit dual-ladder R-string DAC with 4-bit MSB ladder

Initially, the performance of a 10-bit dual-ladder R-string DAC with a 4-bit MSB ladder will be considered. This structure is defined by the parameters n_1=4 and n_2=6 in the variance of INL_m given in equation (22). This variance is dependent upon the total area, A_{TOT}, and the process parameter $A_{\rho N}$. By normalizing the variance by $A^2_{\rho N}/A_{TOT}$, the effects of x,z, and m on the INL_m can be practically depicted. With this normalization, (33) simplifies to

$$\sigma^2_{NORM}(INL_m) = 2^{n1}\left[\frac{z^2}{x}+\frac{(1-z)^2}{(1-x)}\right]\left[\left(2^{n_2}-p\times 2^{n_2-n_1}-q\times 2^{-n_1}\right)^2 p+\left(q-p\times 2^{n_2-n_1}-q\times 2^{-n_1}\right)^2\right] + \left(p\times 2^{n_2-n_1}+q\times 2^{-n_1}\right)^2 (2^{n_1}-p-1)\Big]+\frac{2^n}{(1-x)}\left[q\left(1-q\times 2^{-n_2}\right)^2+q^2\times 2^{-2n_2}\left(2^{n_2}-q\right)\right] \quad (70)$$

where x, z, and m are as defined in (17), (18) and (25).

The normalized standard deviation of the INL_m for x and z $\in$ {0.01, 0.5, 0.95} are shown in Figure 9, 10, 11. From these plots, it is apparent that the INL assumes a maximum near the mid-code tap voltage corresponding to code 512. Consistent with Figure 4, it can be seen from Figure 9 that the maximum normalized standard deviation for x = z = 0.01 is very close to the global minimum of 1. The plot of Figure 9 which is for x small corresponds to the situation where most of the area is allocated to the fine resistors. Figure 10, where x = 0.5, corresponds to the situation where equal area is allocated to the coarse and fine resistor strings whereas Figure 11, where x=0.95 represents the situation where most of the area is allocated to the coarse string.

In Figure 9, when z is large, the voltage at the taps of the coarse string plays the major role in the nonlinearity and since the area of the coarse resistors is small, there is a large variance in the coarse tap voltages and that causes the INL to be large throughout most of the output voltage taps. Correspondingly, in the same figure, when z is small, the impedance at the coarse string plays only a small role in determining the overall INL and since most of the area is allocated to the fine string, the INL is very good.

In Figure 11, when z is large, the impedance at the taps of the coarse string plays a major role in the nonlinearity and since the area of the coarse resistors is large, there is a small variance in the coarse tap voltages that causes the INL at the tap voltages to be small for most of the coarse voltage taps. But since there is little area in the fine resistors, the

variance in the voltage at intermediate nodes in the fine string gets rather large. Correspondingly, when z is small, the impedance at the taps of the fine string plays a major role in the nonlinearity and since the area of the fine resistors is small, the variance is large at most of the fine output voltage taps.

It is apparent from these plots that under certain conditions, there is considerable "ripple" in the INL. This ripple occurs when the relative area in the fine string is small (z is large). When the ripple is present, the local maxima and the local minima occur at coarse ladder taps or at mid tap locations of the fine ladder depending upon how the resistance and area is allocated. There are a total of 2^{n_1+1} critical tap points in the array.

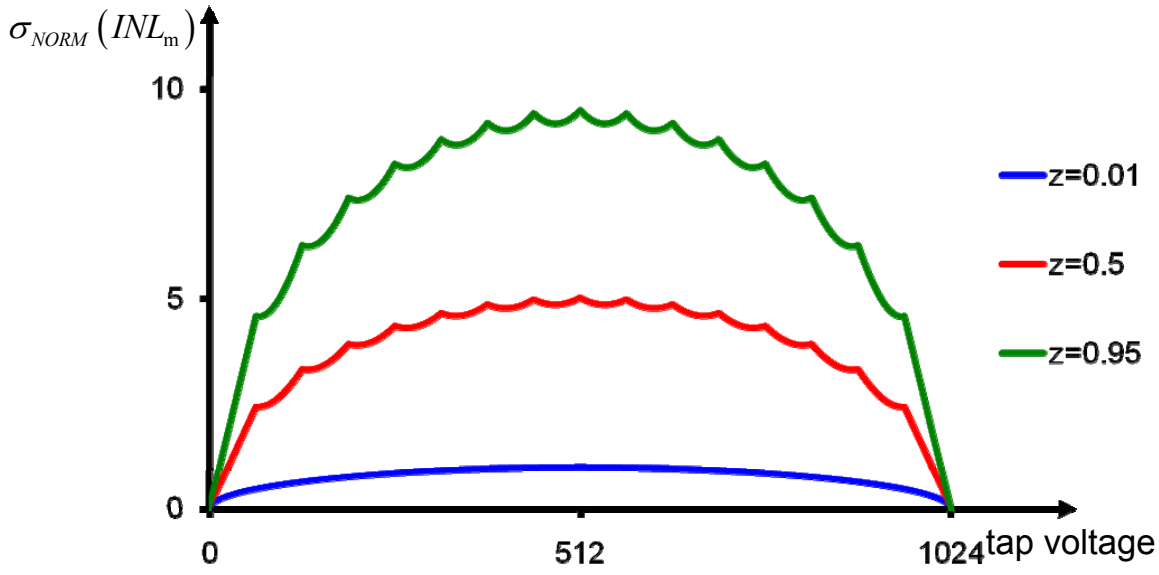

Figure 9. INL profiles of the dual ladder DAC for x = 0.01

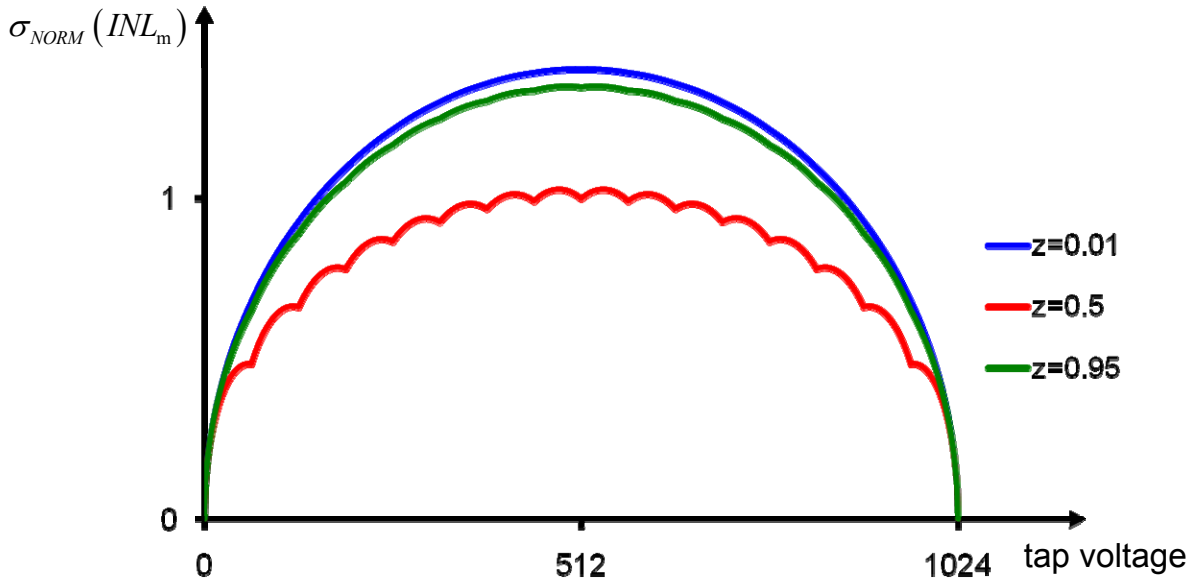

Figure 10. INL profiles of the dual ladder DAC for x = 0.5

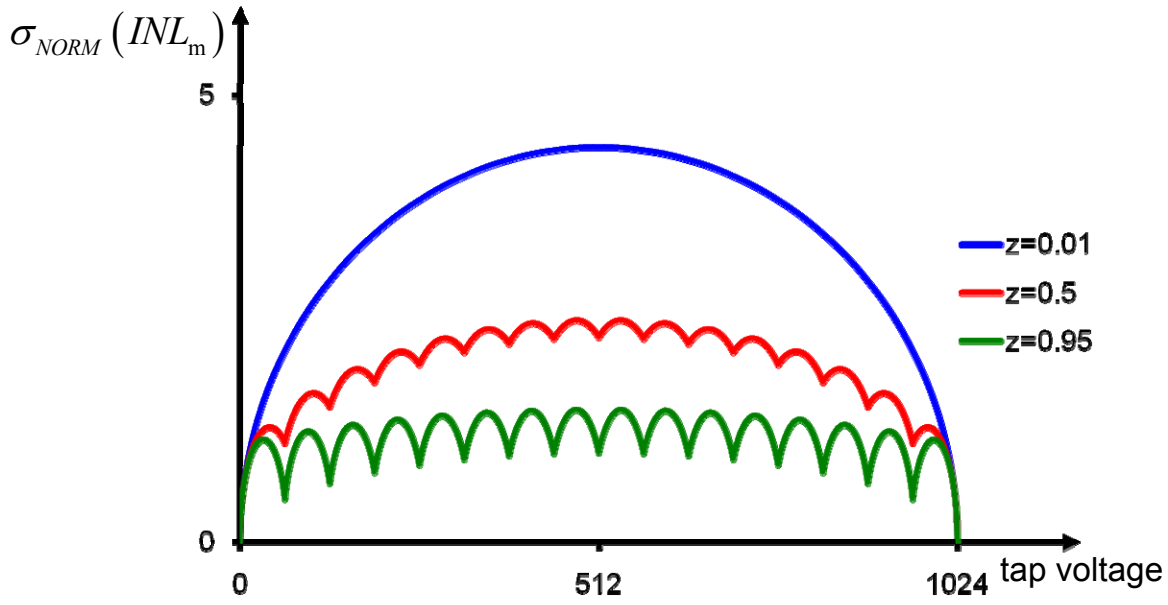

Figure 11. INL profiles of the dual ladder DAC for x = 0.95

It can also be seen that the INL deviation increases with |x – z| and when |x – z| is small, it reduces when x and z move closer to the origin. Simulation results of the maximum INL standard deviations are summarized in the Table 2.

Table 2. Simulation results of $\sigma_{\max-NORM}$

z	x=0.01		x =0.5		x= 0.95	
	$\sigma_{\max\text{-}NORM}(INL_m)$	Δn_{EQ}	$\sigma_{\max\text{-}NORM}$ (INL_m)	Δn_{EQ}	$\sigma_{max\text{-}NORM}$ (INL_m)	Δn_{EQ}
0.95	9.5	3.3	1.35	0.4	1.5	0.5
0.5	5	2.3	1.03	0.04	2.5	1.3
0.01	1	0	1.4	0.5	4.4	2.2

Simulation results show that when x and z are small, for example, x = z = 0.01, the normalized maximum standard deviation, $\sigma_{\max-NORM}$,is approximately 1 and moving closer to the origin on the x = z line does not reduce the standard deviation appreciably below 1. Also shown in Table 2 is Δn_{EQ}, the effective number of bits of resolution lost relative to what would be achieved with an optimal area/impedance allocation. When choosing x = z to attain the minimum standard deviation for a fixed x, the effective number of bits (ENOB) merely reduces by 0.04 bits when x = z = 0.5 and reduces by 0.5 bits when x = z = 0.95. However, if x is in the neighborhood of 1 and z in the neighborhood of 0 or vice versa, then the standard deviation will be very large. For example, in the case x =0.95, z = 0.01, the ENOB reduces by 2.2 bits and in the case x= 0.01, z = 0.95, the ENOB reduces by 3.3 bits. It should be apparent that the implications of a non-optimal area/impedance allocation can have a dramatic impact on the yield of a DAC if the deviation from the optimal x = z line is large.

Figure 12 shows the effects of different allocations of impedance and area throughout the x-z plane from a different perspective. The continuous loci on this plot correspond to iso-area contours and are labeled in terms of the increase in area needed to obtain a standard deviation equal to that obtained at the optimal point x = z = 0. This provides some insight into the area penalty incurred to obtain the same yield if non-optimal area and impedance

allocations are used. For example, the point x = 0.1 and z= 0.7 lies on the 400% area contour indicating that a factor of 4 increase in area is required to obtain the same yield as would be obtained for an optimal area/impedance allocation.

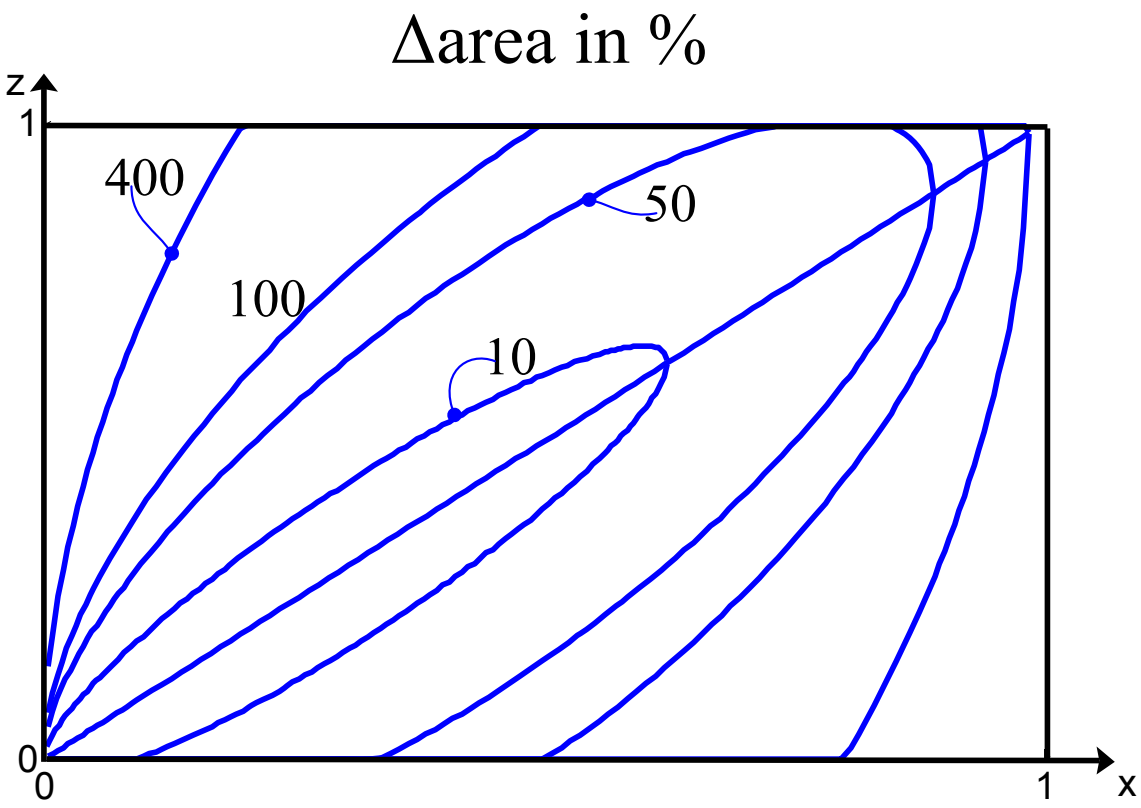

Figure 12. Increasing Area to achieve the same INL

The parameters x and z, as defined in (17) and (18) may partially obscure the relative effects of area and impedance on yield. The effects of non-ideal impedance and area allocation is shown in the $\log(R_F/R_C)$ – x plane in Figure 13 where again the iso-area contours are used. As an example, to maintain the same yield as in the optimal case, when the area of the coarse string is equal $\frac{1}{10}$ of the total area, the total area increases by 10% if $R_C = 4R_F$, it increases by 50% if $R_C = 2.2R_F$, and it increases by more than 400% if $R_C = 2.3R_F$.

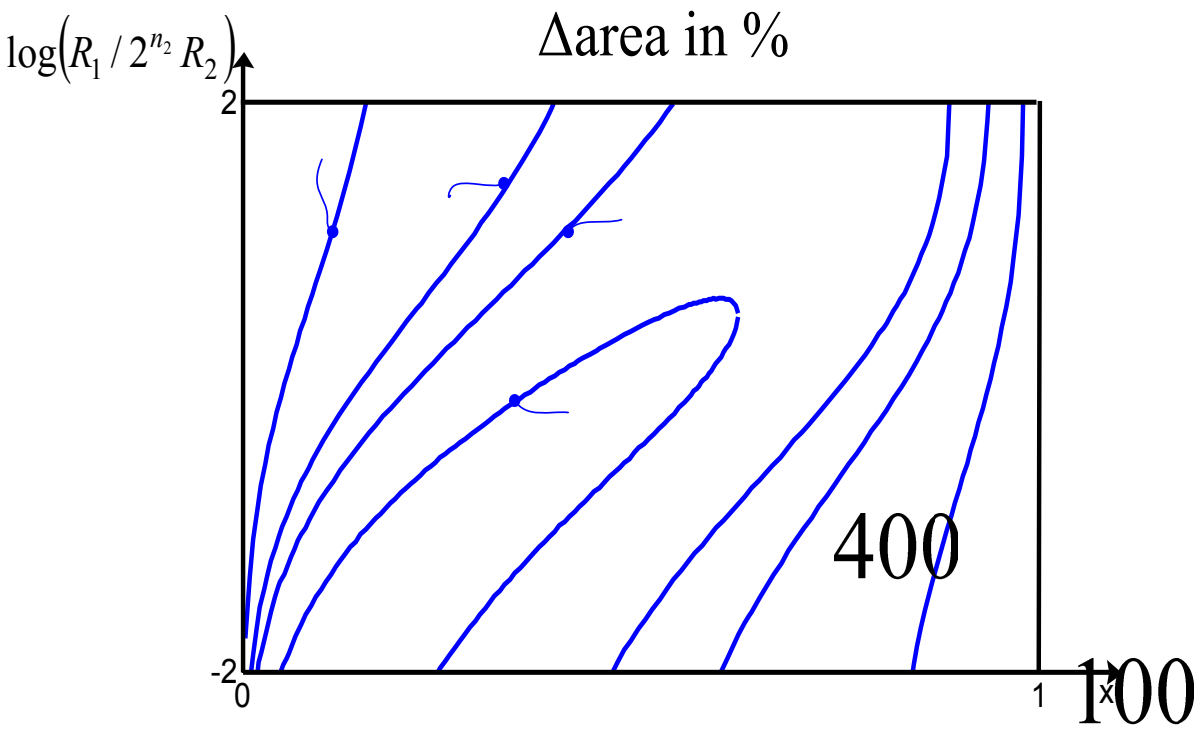

Figure 13. Effect of selection of impedance and area

3.1.2 Simulation results for different values of n and n_1

A comparison of the maximum standard deviation of the INL_m for different n – bit DAC area and impedance partitioning strategies for the dual ladder DAC is also made. In this comparison, it will be assumed that the DAC have the same values of the total area and the total impedance for all n. A Matlab program was used for calculating the standard deviation of INL in the limiting case: x = z, and x -> 0 for different values of n and n_1. This limiting case forms a tight lower bound on the standard deviation of the INL. The point (0,0) in the x-z plane is not realizable since it does not lie in the open unit square but values of x and z can be selected in the open unit square that are arbitrarily close to this point. These results show that the lower bound is strongly dependent upon n but independent of n_1. The results are summarized in the Table 3.

Table 3. The optimum $\sigma_{NORM}(INL_m)$ of the dual ladder DAC as n varies

N	4	5	6	7	8	9	10	11	12
$\sigma_{NORM}(INL_m)$	1	1	1	1	1	1	1	1	1

Additional simulation results for different values of x and z are included in Appendix A and Appendix B. It is seen that the effective number of bits (ENOB) reduces very slightly when (x,z) moves away from (x=0, z=0) on the locus x=z as indicated in the Theorem 4. However, ENOB reduces significantly for the case z=1-x.

3.2 Interpretation of $\sigma^2_{INL_m}$ for Interpolation with buffer

In this section, the performance of the Interpolation DAC with buffer is characterized mathematically by the equation (44) in the section 2.3.

3.2.1 Simulation results for n =10

To interpret the analysis presented in Section 2.3, graphical results of an interpolation DAC with $n_1 = 4$, n=10 were characterized by equation (44) to compare the performance for a variety of impedances and layout area allocations.

INL profile curves are in Figure 14 when x is 0.1, 0.5 and 0.94543 and 0.99, respectively. For each value of x, the INL profile looks like a ripple on which the local maxima and the local minima occur at coarse ladder taps and in mid taps of the fine ladders. Thus, there are total 2^{n_1+1} critical taps. The maximum variance happens at a sub-tap of the fine string located in the neighborhood of the middle tap, dependent on the impedance / area allocations.

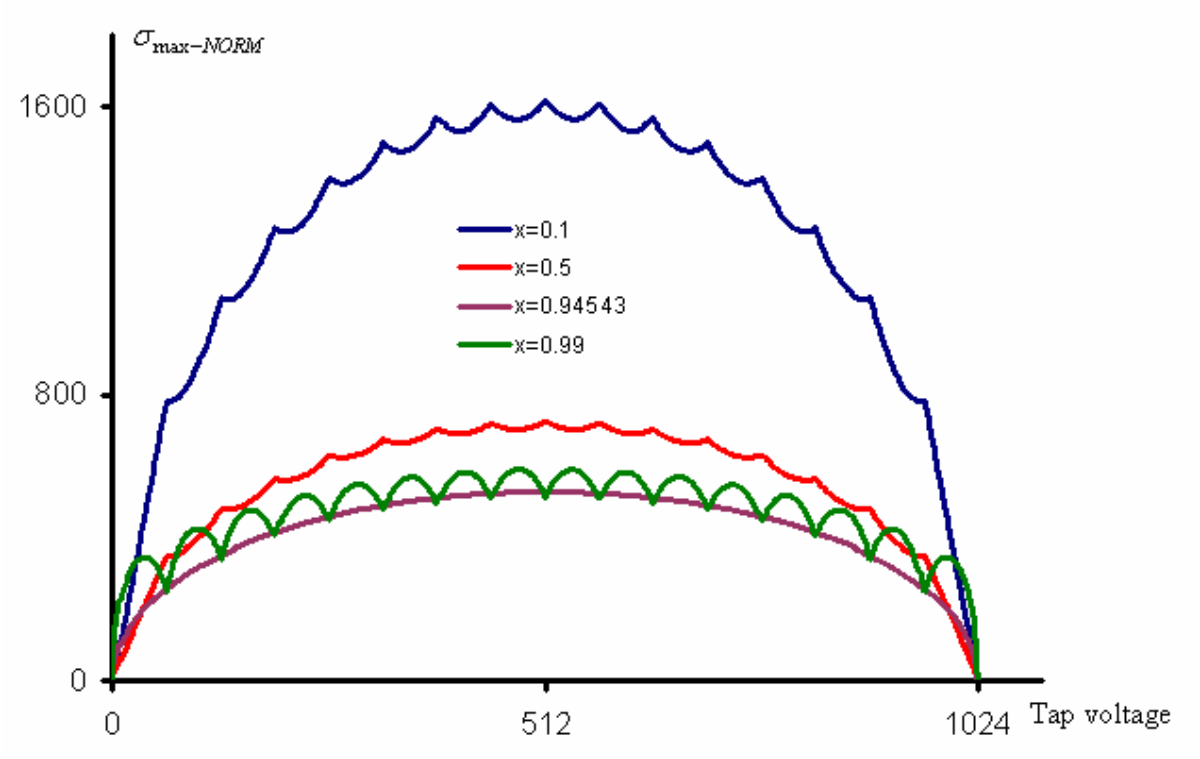

Figure 14. $\sigma_{max-NORM}$ **w.r.t the voltage position tap n=10, n1 =4**

The variance of INL is denoted by $\sigma^2_{INL_m}$ in (30) is a function of 5 variables, the ratio of area x, the number bits on the coarse string n_1, the number bits on the fine string n_2, the tap position on the coarse string p, and the tap position on the fine string q. Analytical expression for statistical of INL such as the optimum value of σ_{INL_m} is not mathematically implemeted. However, this information is very necessary for predicting the linear performance of the circuit as wel as knowledge of efficent designs. Therefore, computing simulations were used for guessing the criticals values of σ_{INL_m}.

Figure 15 is the standard deviation σ_{INL_m} using a Matlab program. It is clearly that the minimum of the standard deviation σ_{INL_m} obtained if the ratio x = $\left(\frac{2^{n_1} A_1}{A_{TOT}}\right)$ is around 0.95.

Otherwise, if most of area is used for layout fine resistors, the standard deviation σ_{INL_m} will increase more than 2 times for x smaller than 2.5.

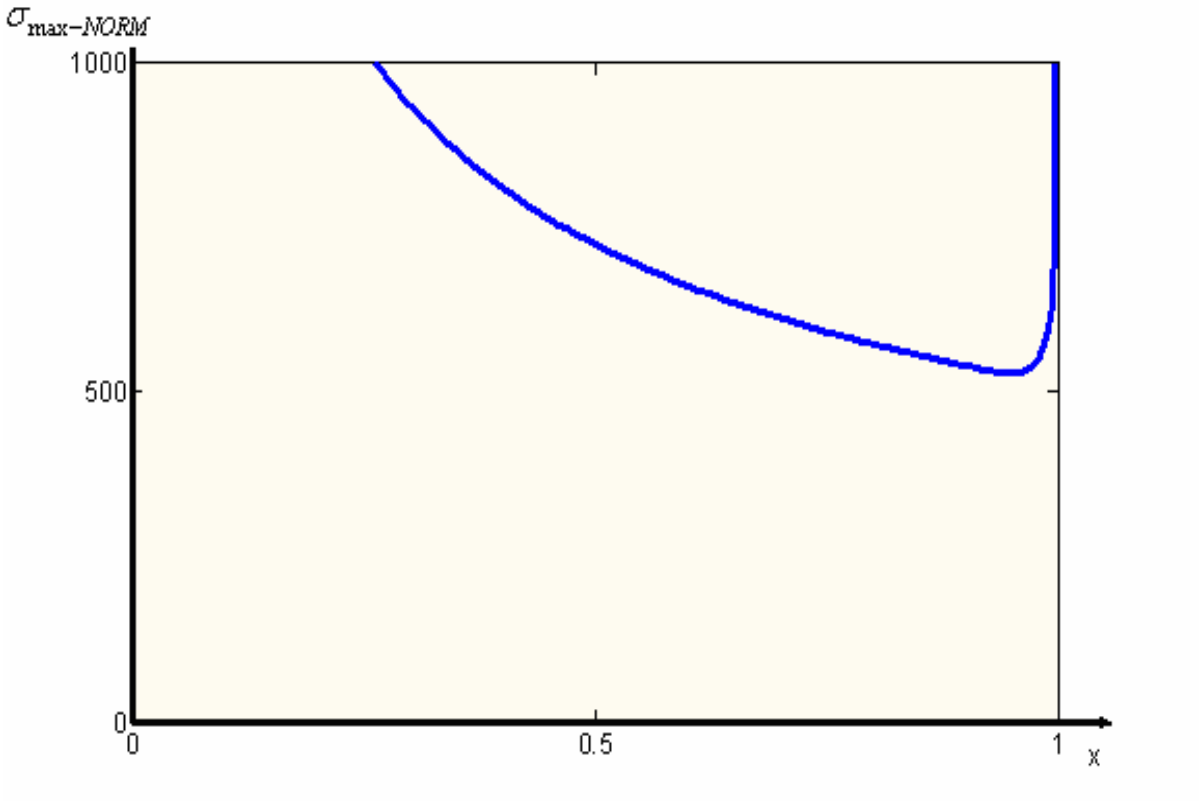

Figure 15. $\sigma_{max-NORM}$ **w.r.t x for n_1 =4, n_2 = 6**

A comparison of the standard deviation of the INL for different values of the number bits on the coarse ladder n_1 is simulated. Figure 16 show that if increasing the number bits on the coarse ladder string, the standard deviation σ_{INL_m} will decrease. The compensation of this benefits is the complexity of the coarse string layout.

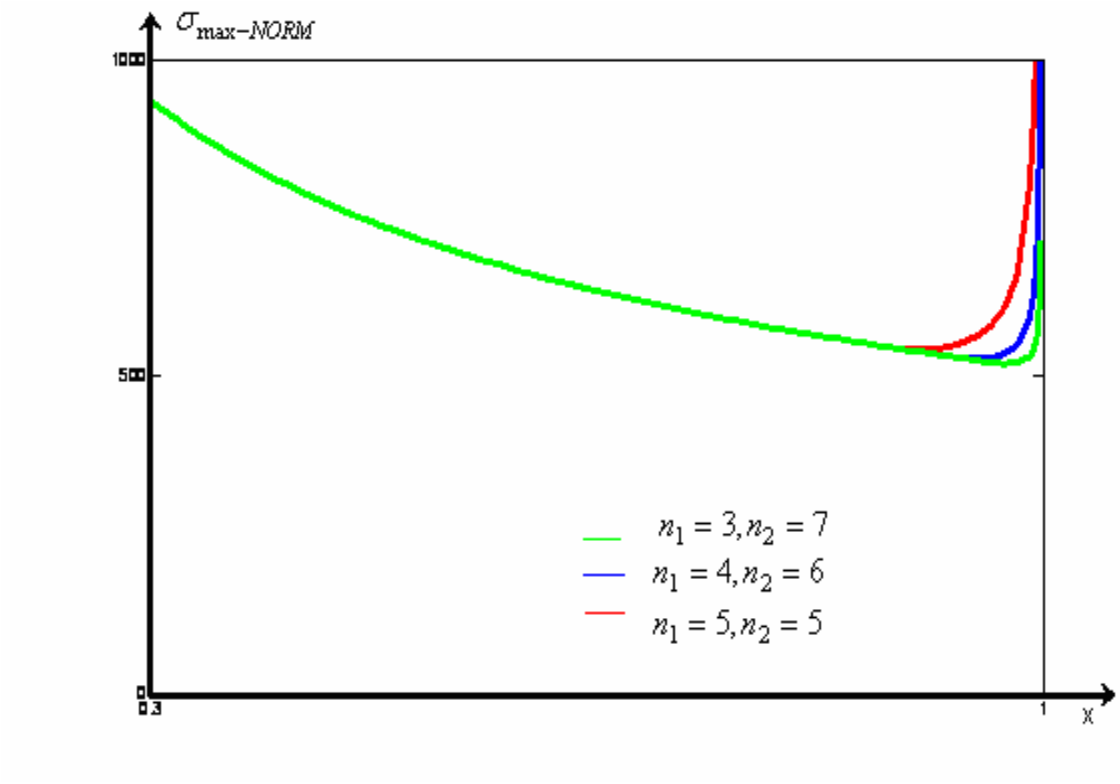

Figure 16. $\sigma_{max-NORM}$ **w.r.t**. x for n_1 = 3, 4, 5

3.2.2 Simulation results for different value of n and n_1

A comparison of the maximum standard deviation of the INL for the conventional n – bit DAC area and impedance partitioning strategies for the dual ladder DAC is also made. In this comparison, it will be assumed that the DAC have the same values of the total area and the total impedance for all n. A Matlab program was used for calculating the minimum values the standard deviation of INL and the critical ratio $x=\left(\frac{2^{n_1} A_1}{A_{TOT}}\right)$. The results are summarized in the Table 4.

Table 4. The minimum of Standard deviation of INL and x to obtain the minimum value of the standard deviation of the INL

n1 / n		2	3	4	5	6	7	8	9	10
4	$\sigma_{\max-NORM}$	8.9								
	x	0.82								
5	$\sigma_{\max-NORM}$	17.8	16.9							
	x	0.82	0.9							
6	$\sigma_{\max-NORM}$	35.6	33.7	33						
	x	0.82	0.9	0.95						
7	$\sigma_{\max-NORM}$	71.1	67.7	66	65					
	x	0.82	0.9	0.95	0.97					
8	$\sigma_{\max-NORM}$	142	135	132	130	129				
	x	0.82	0.9	0.95	0.97	0.99				
9	$\sigma_{\max-NORM}$	285	271	264	260	258	257			
	x	0.82	0.9	0.95	0.97	0.99	0.99			
10	$\sigma_{\max-NORM}$	569	542	528	520	517	515	515		
	x	0.82	0.9	0.95	0.97	0.99	0.99	0.99		
11	$\sigma_{\max-NORM}$	1138	10834	1055	1040	1033	1029	1029	1029	
	x	0.82	0.9	0.95	0.97	0.99	0.99	0.99	0.99	
12	$\sigma_{\max-NORM}$	2276	2167	2110	2080	2067	2058	2058	2058	2058
	x	0.82	0.9	0.95	0.97	0.99	0.99	0.99	0.99	0.99

Increasing the resolution of the DAC will increase the standard deviation of the INL. In all cases, the wise strategies are placing most of the area on the coarse string, only 20% of the total area is used for the fine string layout.

3.3 Interpretation of $\sigma^2_{INL_m}$ for Interpolation with buffer resistors

The performance interpretation of interpolation with buffer resistors of Figure 8 is investigated in this section by the formula of $\sigma^2_{INL_m}$ given by equation (69) in the section 2.4.

3.3.1 Simulation results for n =10

To interpretate the analysis presented in 2.4, graphical results of an interpolation DAC with buffer resistors for $n_1 = 4$, n=10 were brought out to compare the performance of variety of impedances and layout areas allocation. The variance in the equation (69) is dependent on the total area, A_{TOT}, and the process parameter, $A_{\rho N}$. By normalizing the variance by $A^2_{\rho N}/A_{TOT}$, the effects of z, and m on the INL_m can be practically depicted. With this normalization, (69) simplifies to $\sigma_{\max-NORM}$

$$\sigma^2_{NORM}(INL_m) \approx 2^{n_1} M_1 \frac{z^2}{a_1} + 2^{n_1} M_2 \frac{(1-z)^2}{a_3} + M_3 \frac{(1-z)^2}{a_2} + M_4 \frac{1}{a_2} \qquad (71)$$

INL profile curves are in Figure 17 and Figure 18 for the case z=0.1 and z=0.9 respectively. For each case, the INL profile looks like a ripple on which the local maxima and the local minima occur at coarse ladder taps and in mid taps of the fine ladders. The maximum standard deviation position is dependent on the impedance / area allocations.

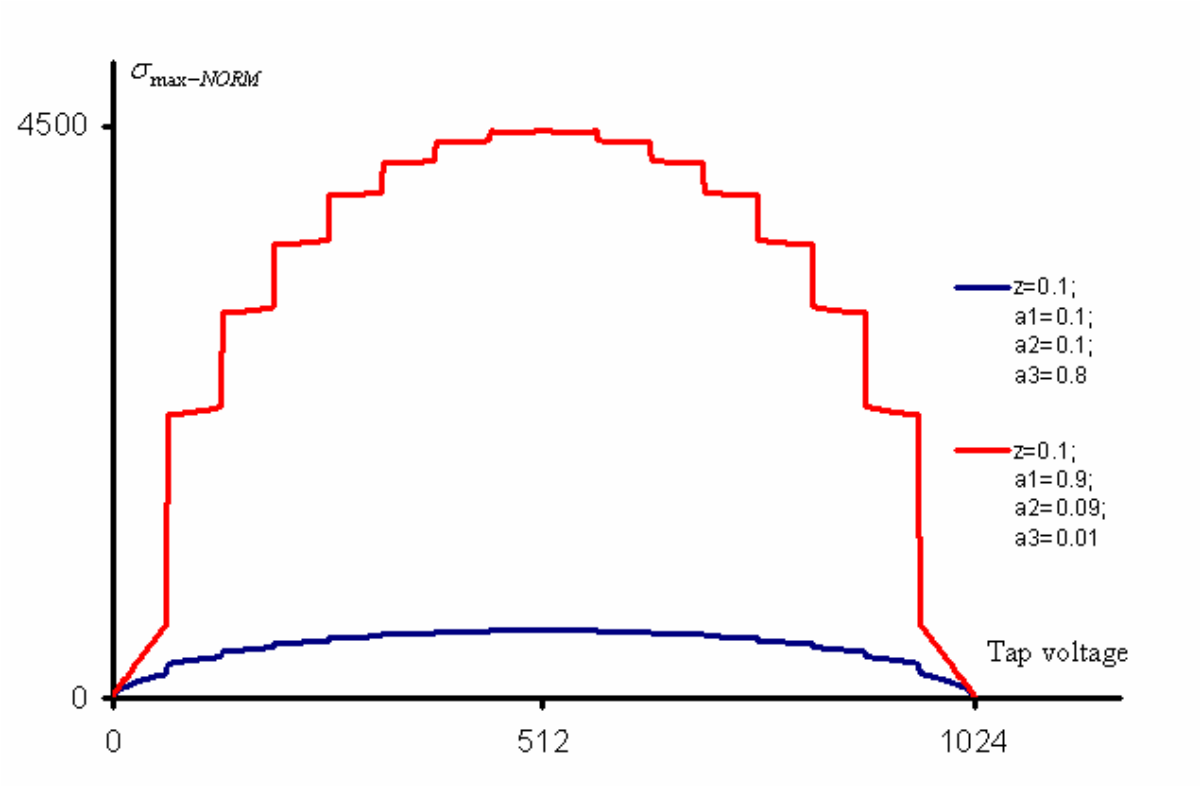

Figure 17. The standard deviation profile for z=0.1

From Figure 17, the maximum standard deviation of the red curve placing most the area on the coarse string while a small area on the fine string and buffer resistors is bigger 9 times than the maximum standard deviation of the blue curve placing most the area on buffer resistors while a small area on the fine string and the coarse string.

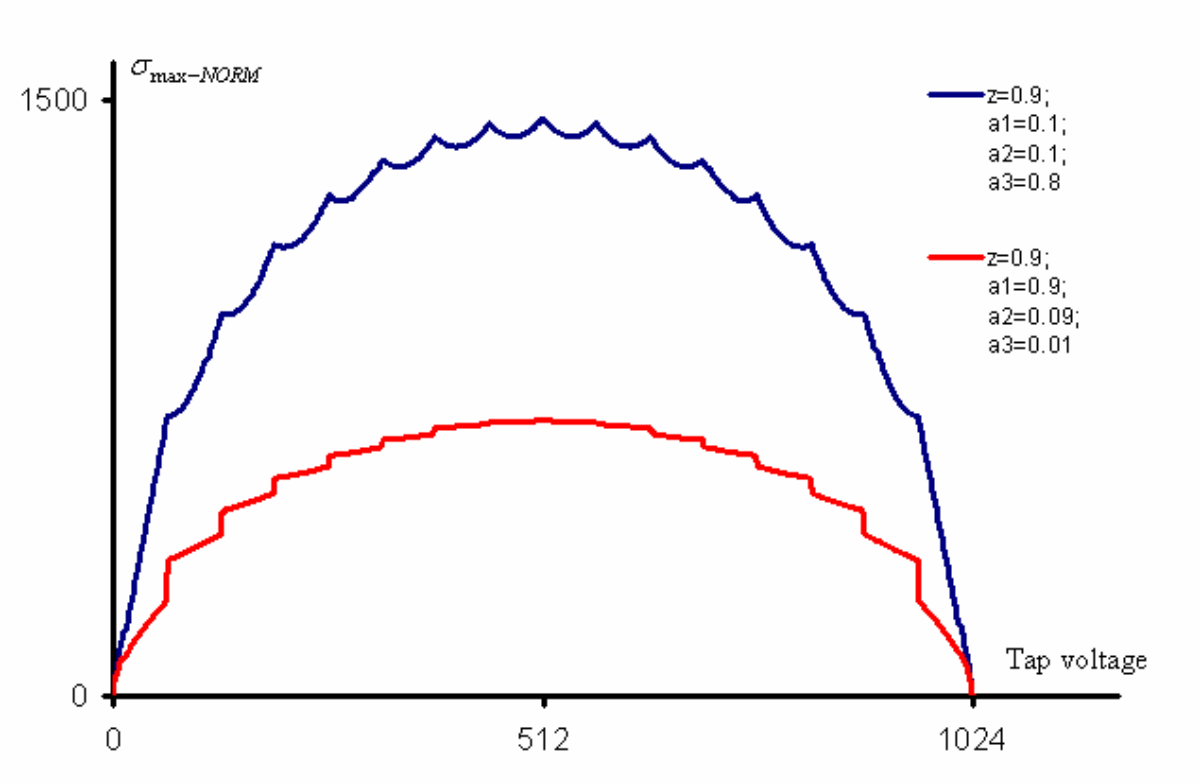

Figure 18. The standard deviation profile for z=0.9

On the other hand, in the Figure 18 for the case z= $\frac{R_{TOT}}{2^n R_1}$ large, the maximum standard deviation of the red curve placing most the area on the coarse string while a small area on the fine string and buffer resistors is smaller 2 times than the maximum standard deviation of the blue curve placing most the area on buffer resistors while a small area on the fine string and the coarse string.

These two examples raise a question what is the optimum area and impedance allocation between the coarse resistors, the fine resistors and the buffer resistors. The equation to calculate the standard deviation in (69), (71) is a function of 4 variables: the ratio resistor z, the ratio of areas a_1, a_2, a_3. If we can indicate the region of the optimum, the cost of the DAC design will lower by reducing the dice area to achieve the same yield. However, it

is impossible to obtain the mathematical expressions for the optimal area and impedance allocation. Computer simulations can be used for obtaining neiborhood regions of the optimum positions.

Table 5 is results of simulations in Matlab. It is clear that to the ratio of the coarse string area to the total area is approximately equal to the ratio of the total resistance to the coarse string resistance while most of remaining area is placed on the buffer resistors.

Table 5. The optimum values of $\sigma_{max-NORM}$ for n=10, n_1 =4

z	a_1	a_2	a_3	The optimum of $\sigma_{max-NORM}$
0.1	0.1	0.09	0.81	530
0.2	0.2	0.09	0.71	530
0.3	0.3	0.09	0.61	531
0.4	0.4	0.09	0.51	532
0.5	0.5	0.09	0.41	533
0.6	0.6	0.09	0.31	535
0.7	0.6	0.09	0.21	535
0.8	0.7	0.09	0.11	536
0.9	0.8	0.09	0.01	537

3.3.1 Simulation results for different values of n

A comparison of the standard deviation of the INL for the conventional different n – bit DAC area and impedance partitioning strategies for the dual ladder DAC is also made. In this comparison, it will be assumed that the DAC have the same values of the total area and

the total impedance for all n. A Matlab program was used for calculating the standard deviation of INL in the position near the optimum points. The results are summarized in the Table 6.

Table 6. The average values of $\sigma_{max-NORM}$

n1 / n	2	3	4	5	6	7	8	9	10
4	8.8								
5	17.7	17							
6	35	34	33						
7	70	68	67	66					
8	140	136	132	132	133				
9	281	272	265	266	268	268			
10	563	543	530.4	531.1	533.7	535.2	536.5		
11	1123	1086	1061	1063	1067	1071	1072	1073	
12	2246	2173	2121	2126	2135	2141	2144	2146	2147

It is apparently that the standard deviation σ_{INL_m} increases with the number bits of DAC by nearly a factor of $2^{\Delta n}$. Furthermore, increase the number bits on the coarse string is not the efficient way to enhance the linear performance of the DAC. It is shown that the standard deviation σ_{INL_m} is nearly constant if the areas and impedances are allocated in a wisdom way. The data related to the area and inpedance allacation is in the Appendix C.

CHAPTER 4. ASSESSMENT OF PRIOR WORKS AND VALIDATION OF ANALYTICAL RESULTS

Although use of the dual-string DAC to manage gradients is a useful and well-known technique, there is little in the literature that addresses how area should be allocated between the coarse string and the fine string or how the relative impedances between the coarse string and the fine string should be chosen. The results derived in Chapter 2 and interpreted in Chapter 3 show that the benefits of optimally allocating area and impedance can be most significant. In fact, there is little in the literature to suggest that most designers are even aware of the importance of considering area allocation and impedance assignment when designing dual-string DACs. In this chapter, an attempt will be made to assess the effectiveness of area allocation and impedance allocation in one of the few papers that provides enough information to make an assessment.

The analytical expressions for the variance presented in Chapter 2 are quite complicated and considerable manipulative details were necessary to obtain these closed-form expressions. The question naturally arises about whether any errors were made in these derivations. A key component of these derivations was the linearization of the random variables that appeared in tap voltages and the INL expressions. This linearization was necessary to obtain a mathematically tractable expression for the variance of a function that was dependent upon a large number of random variables that were assumed to be uncorrelated. The question of how much error was introduced in these linearizations also naturally arises. Although it is difficult to verify that no errors were made in the analytical derivations or separate possible errors in the derivations from errors introduced by the

linearizations, statistical simulations of special cases of the dual-string DAC can be made and the results can be compared with the analytical results developed in Chapter 2. If close agreement between the simulated results and the analytical formulations is demonstrated, a reasonable level of confidence can be established that the analytical results correctly predict the performance of a dual-string DAC. In this chapter, statistical simulations are used to validate the analytical results presented in Chapter 2.

4.1 Assessment of Published Results

One of the few, if not the only, published results that provide enough details about the impedance and area allocations in the dual-ladder structure to assess the performance relative to the optimal area and impedance allocations came out of Phillips. This highly cited work was initially published by Pelgrom [Pelgrom, M. J. M. (1990)] and discussed more generally in a book by van de Plassche [Plassche, R. van de (2003)]. This work focused on a 10-bit DAC using the basic architecture of Figure 3. In this work, 4 bits were allocated to the coarse string. The 16 coarse resistors, placed in a common-centroid layout using an antiparallel structure, were each nominally 125 Ω. The fine string resistors were each nominally 75 Ω. Although the area allocation to the coarse and fine resistors in [Pelgrom, M. J. M. (1990)] was not given, a die photograph showed that the total area for the fine resistor string was approximately 7 times that for the coarse string. This total area for both the coarse array and the fine array includes the area required for resistor separation, contact placement, switch connections, and other layout considerations. The assumption will be made that the actual area ratios for the coarse and fine resistors is close to the total area ratio. For convenience, it was assumed that the fine area / coarse area ratio is 6.87. Thus, using the terminology of

Section 2.2, the experimental structure reported by Pelgrom is assumed to be characterized by the parameters n = 10, $n_1 = 4$, x = 0.13, z = 0.97. This point, designated as [Pelgrom, M. J. M. (1990)], is shown on the unit square in the x – z plane in Figure 19. It is apparent that this point is not close to the x = z locus and not close to the Lower Variance Bound (LVB). It can be seen from Figure 13 that since this point is so far removed from the x = z locus, the variance will be much larger than that achievable near the LVB point..

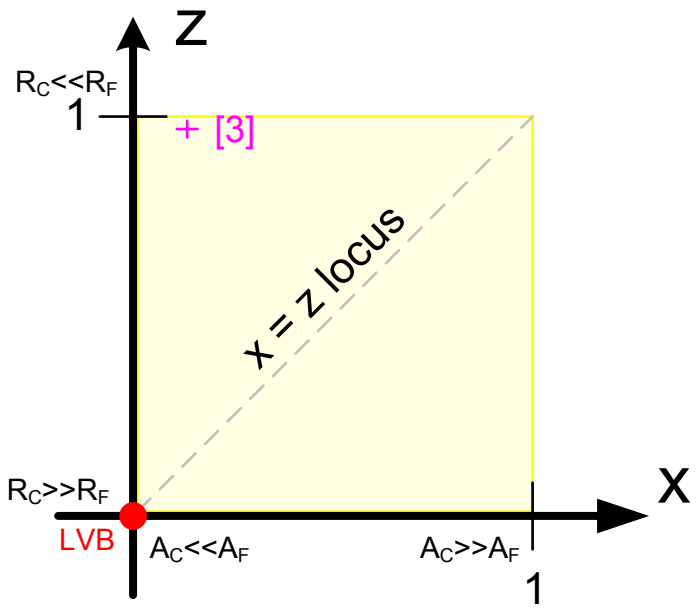

Figure 19. Characterization of design reported in [Pelgrom, M. J. M. (1990)] in the x-z plane

Although there is not enough resolution in Table 12 to determine the actual area penalty associated with the non-optimal point (0.13, 0.97), using the results of Sec. 2.3, it can be shown that the area could be reduced by a factor of 7 with a near optimal impedance assignment even if the relative areas remain unchanged by moving to the point (0.13, 0.13) on the x = z line while maintaining the same yield. Alternatively, while maintaining the same

yield, the area could be reduced by a factor of 5 by operating at the point x = 0.793, z = 0.986 or by a factor of 6 by operating at the point x = 0.712, z = 0.789.

4.2 Validation of INL variance formulation

The closed-form expressions for the output voltage of the DAC and correspondingly the variance of INL_m such as those given in (33) and (34) of Chapter 2 are useful for engineers when designing and laying out the basic R-String DACs. However, considerable arithmetic operations were required to obtain these expressions and these arithmetic operations included making approximations that were based upon the assumption that that random component of the resistances is small compared to the nominal component. The question of whether any errors occurred in the derivations or whether the approximations are justifiable naturally arises. In this section we will attempt to validate the approach by comparing the analytical results with those obtained with an independent statistical simulation for a specific example.

In this statistical simulation, 10,000 dual string 10-bit DACs were randomly generated with MATLAB code. Each DAC had 4 bits in the coarse string. The area and impedance allocations were selected to agree with those of [Pelgrom, M. J. M. (1990)], specifically (x = 0.13, z = 0.97). In this simulation, it was assumed that the resistors came from a truncated normal distribution characterized by $\frac{A_{\rho N}}{\sqrt{A_{ToT}}} = 1.26E-3$. The truncation was used to throw out any resistor that deviated by more than 1% from the nominal value. Figure 20 shows a plot of INL profile obtaining from thus statistical simulation and compares results with those obtained from (33). From this plot, it is apparent that the analytical formulation of (33) is in close agreement with the statistical MATLAB simulation.

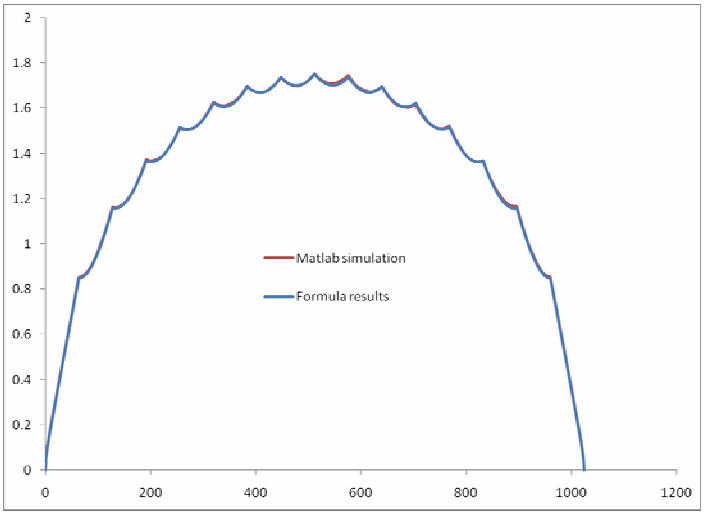

Figure 20. The standard deviation profiles for Pelgrom case

Similary, simulations of a sample population of 10,000 randomly generated DACs were also were run for the case x = 0.793, z = 0.986 and x = 0.712, z= 0.789 to compare with the results obtained from the formula (33). The results are shown in Figure 18 and Figure 19. Again, it can be seen that there is very close agreemnt between the analytical results of (33) and those obtained with the statistical MATLAB simulations.

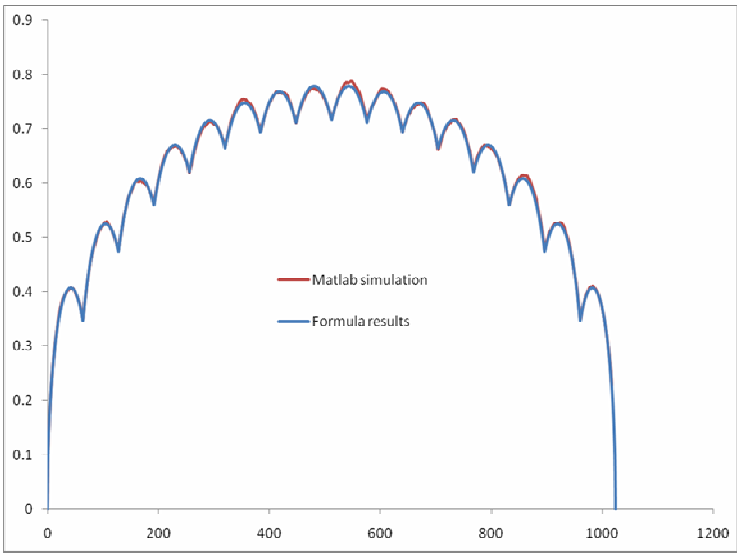

Figure 21. The standard deviation profiles for the case x=0.793, z=0.986

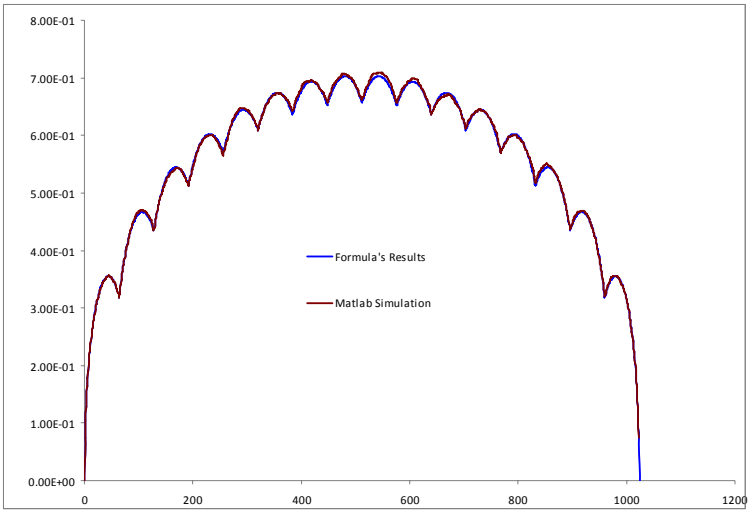

Figure 22. The standard deviation profiles for x=0.712, z=0.789

Although these three statistical simulations do not prove that the analytical results of (33) are correct, the close agreement between the simulated results and the analytical formulation provides a high level of confidence that the analytical formulations are valid.

CHAPTER 5. CONCLUSIONS

The effects of random variations in sheet resistance on the linearity performance of three different dual-ladder resistor string DACs were analytically characterized. A formulation of the INL was presented. The relation between linearity, area allocation, and impedance allocation were discussed and optimal area and impedance allocation strategies were presented.

For the basic dual ladder DAC, optimal yield for a given total resistor area is achieved when the ratio of the coarse string area to the total area equals the ratio of the total resistance of the DAC to the coarse string resistance.

For the dual ladder with buffer, the impedance and area allocation strategies for maximizing yield with a given total resistor area are quite different. . In this case, optimal performance requires allocating a higher percentage of the total area to the coarse string whereas the impedance allocation does not affect linearity performance.

Finally, the impedance and area allocating strategies of the dual ladder with buffer resistors represents a higher-order system where closed-form expressions for optimal area and impedance allocations are more difficult to derive. Simulation results suggest that impedance allocations comparable to that for the basic dual-string DAC will provide reasonably good performance and that most area should be allocated to the coarse string and the interpolation resistor with proportionally smaller area being allocated to the replacement resistors. .

In all cases, it has been shown either by analytical derivations or computer simulations that dramatic improvements in yield for a given total resistor area can be

obtained by using optimal or near optimal impedance and area allocation strategies for assigning impedance and area in dual-string DACs. Equivalently, dramatic reductions in total resistor area for a given yield target can be obtained with optimal or near optimal impedance and area allocation strategies when compared to what is achievable with intuitive but non-optimal approaches. Invariably, paralleling the reduction in cost associated with reducing resistor area will be an improvement in speed and a reduction in power since the relative parasitic capacitances will invariably be reduced when area is reduced.

APPENDIX A. $\sigma_{\max-NORM}$ OF DUAL LADDER DACS FOR X=Z

Table 7. $\sigma_{\max-NORM}$ **for n =4**

x=z / n_1	0.01	Δn_{EQ}	0.1	Δn_{EQ}	0.5	Δn_{EQ}	0.9	Δn_{EQ}	0.99	Δn_{EQ}
1	1		1	0.005	1.15	0.2	2.25	1.2	7.13	2.8
2	1		1	0.004	1.09	0.1	1.75	0.8	5.13	2.4

Table 8. $\sigma_{\max-NORM}$ **for n =5**

x=z / n_1	0.01	Δn_{EQ}	0.1	Δn_{EQ}	0.5	Δn_{EQ}	0.9	Δn_{EQ}	0.99	Δn_{EQ}
1	1		1	0.0063	1.15	0.21	2.31	1.21	7.06	2.82
2	1		1	0.0054	1.1	0.13	1.81	0.86	5.06	2.34
3	1		1	0.0045	1.06	0.08	1.44	0.52	3.63	1.86

Table 9. $\sigma_{\max-NORM}$ **for n =6**

x=z / n_1	0.01	Δn_{EQ}	0.1	Δn_{EQ}	0.5	Δn_{EQ}	0.9	Δn_{EQ}	0.99	Δn_{EQ}
1	1		1.01	0.007	1.15	0.21	2.3	1.2	7.09	2.83
2	1		1	0.006	1.1	0.13	1.79	0.84	5.07	2.34
3	1		1	0.005	1.05	0.07	1.45	0.54	3.66	1.87

Table 10. $\sigma_{\max-NORM}$ **for n =7**

x=z / n_1	0.01	Δn_{EQ}	0.1	Δn_{EQ}	0.5	Δn_{EQ}	0.9	Δn_{EQ}	0.99	Δn_{EQ}
1	1		1.01	0.007	1.15	0.21	2.29	1.2	7.09	2.83
2	1		1	0.006	1.1	0.13	1.79	0.84	5.07	2.34
3	1		1	0.005	1.05	0.08	1.45	0.54	3.66	1.87
4	1		1	0.003	1.03	0.04	1.25	0.32	2.69	1.43

Table 11. $\sigma_{\max-NORM}$ **for n =8**

x=z / n_1	0.01	Δn_{EQ}	0.1	Δn_{EQ}	0.5	Δn_{EQ}	0.9	Δn_{EQ}	0.99	Δn_{EQ}
1	1		1.01	0.007	1.15	0.21	2.29	1.2	7.09	2.83
2	1		1	0.006	1.1	0.13	1.79	0.84	5.07	2.34
3	1		1	0.005	1.05	0.08	1.45	0.54	3.65	1.87
4	1		1	0.003	1.03	0.04	1.25	0.32	2.68	1.42

Table 12. $\sigma_{\max-NORM}$ **for n =9**

x=z / n_1	0.01	Δn_{EQ}	0.1	Δn_{EQ}	0.5	Δn_{EQ}	0.9	Δn_{EQ}	0.99	Δn_{EQ}
1	1		1.01	0.007	1.15	0.21	2.29	1.2	7.09	2.83
2	1		1	0.006	1.1	0.13	1.79	0.84	5.07	2.34
3	1		1	0.005	1.05	0.08	1.45	0.54	3.66	1.87
4	1		1	0.003	1.03	0.04	1.25	0.32	2.68	1.42
5	1		1	0.002	1.02	0.02	1.13	0.18	2.02	1.02

Table 13. $\sigma_{\max-NORM}$ **for n =10**

x=z / n_1	0.01	Δn_{EQ}	0.1	Δn_{EQ}	0.5	Δn_{EQ}	0.9	Δn_{EQ}	0.99	Δn_{EQ}
1	1		1.01	0.007	1.15	0.21	2.29	1.2	7.09	2.83
2	1		1	0.006	1.1	0.13	1.79	0.84	5.07	2.34
3	1		1	0.005	1.05	0.08	1.45	0.54	3.65	1.87
4	1		1	0.003	1.03	0.04	1.25	0.32	2.68	1.42
5	1		1	0.002	1.01	0.01	1.13	0.18	2.02	1.02

Table 14. $\sigma_{\max-NORM}$ **for n =11**

x=z / n_1	0.01	Δn_{EQ}	0.1	Δn_{EQ}	0.5	Δn_{EQ}	0.9	Δn_{EQ}	0.99	Δn_{EQ}
1	1		1	0.007	1.15	0.21	2.29	1.2	7.09	2.83
2	1		1	0.006	1.1	0.13	1.79	0.84	5.07	2.34
3	1		1	0.004	1.05	0.08	1.45	0.54	3.66	1.87
4	1		1	0.003	1.03	0.04	1.25	0.32	2.68	1.42
5	1		1	0.002	1.01	0.02	1.13	0.18	2.02	1.02
6	1		1	0.001	1.01	0.01	1.07	0.1	1.6	0.67

Table 15. $\sigma_{\max-NORM}$ **for n =12**

x=z / n_1	0.01	Δn_{EQ}	0.1	Δn_{EQ}	0.5	Δn_{EQ}	0.9	Δn_{EQ}	0.99	Δn_{EQ}
1	1		1	0.007	1.15	0.21	2.29	1.2	7.09	2.83
2	1		1	0.006	1.1	0.13	1.79	0.84	5.07	2.34
3	1		1	0.005	1.05	0.08	1.45	0.54	3.66	1.87
4	1		1	0.004	1.03	0.04	1.25	0.32	2.68	1.42
5	1		1	0.002	1.02	0.02	1.13	0.18	2.02	1.02
6	1		1	0.001	1.01	0.01	1.07	0.09	1.6	0.67

APPENDIX B. $\sigma_{\max-NORM}$ OF DUAL LADDER DACS FOR Z=1-X

Table 16. $\sigma_{\max-NORM}$ **for n =4**

x / n_1	0.01	Δn_{EQ}	0.1	Δn_{EQ}	0.5	Δn_{EQ}	0.9	Δn_{EQ}	0.99	Δn_{EQ}
1	9.9	3.3	2.86	1.52	1.15	0.2	6.5	2.7	70.13	6.1
2	9.9	3.3	2.86	1.51	1.09	0.1	5.13	2.4	50.13	5.6

Table 17. $\sigma_{\max-NORM}$ for **n =5**

x / n_1	0.01	Δn_{EQ}	0.1	Δn_{EQ}	0.5	Δn_{EQ}	0.9	Δn_{EQ}	0.99	Δn_{EQ}
1	9.9	4.3	2.86	2.52	1.15	1.2	6.53	3.7	70.18	7.1
2	9.9	4.3	2.86	2.52	1.1	1.1	5.08	3.3	50.18	6.6
3	9.9	4.3	2.86	2.51	1.06	1.1	4.13	3	36.19	6.2

Table 18. $\sigma_{\max-NORM}$ **for n =6**

x / n_1	0.01	Δn_{EQ}	0.1	Δn_{EQ}	0.5	Δn_{EQ}	0.9	Δn_{EQ}	0.99	Δn_{EQ}
1	9.9	5.3	2.86	3.5	1.15	2.2	6.53	4.7	70.18	8.1
2	9.9	5.3	2.86	3.5	1.1	2.1	5.08	4.3	50.18	7.6
3	9.9	5.3	2.86	3.5	1.05	2.1	4.14	4	36.18	7.2

Table 19. $\sigma_{\max-NORM}$ **for n =7**

x / n_1	0.01	Δn_{EQ}	0.1	Δn_{EQ}	0.5	Δn_{EQ}	0.9	Δn_{EQ}	0.99	Δn_{EQ}
1	9.9	6.3	2.86	4.52	1.15	3.2	6.53	5.7	70.18	9.1
2	9.9	6.3	2.86	4.52	1.1	3.1	5.08	5.3	50.18	8.6
3	9.9	6.3	2.86	4.51	1.05	3.1	4.14	5.1	36.18	8.2
4	9.9	6.3	2.86	4.51	1.03	3	3.56	4.8	26.53	7.7

Table 20. $\sigma_{\max-NORM}$ **for n =8**

x / n_1	0.01	Δn_{EQ}	0.1	Δn_{EQ}	0.5	Δn_{EQ}	0.9	Δn_{EQ}	0.99	Δn_{EQ}
1	9.9	7.3	2.86	5.5	1.15	4.2	6.53	6.7	70.18	10.1
2	9.9	7.3	2.86	5.5	1.1	4.1	5.09	6.3	50.18	9.6
3	9.9	7.3	2.86	5.5	1.05	4.1	4.13	6	36.19	9.2
4	9.9	7.3	2.85	5.5	1.03	4	3.55	5.8	26.53	8.7

Table 21. $\sigma_{\max-NORM}$ **for n =9**

x / n_1	0.01	Δn_{EQ}	0.1	Δn_{EQ}	0.5	Δn_{EQ}	0.9	Δn_{EQ}	0.99	Δn_{EQ}
1	9.9	8.3	2.86	6.52	1.15	5.2	6.54	7.7	70.18	11.1
2	9.9	8.3	2.86	6.52	1.1	5.1	5.09	7.3	50.18	10.6
3	9.9	8.3	2.86	6.51	1.05	5.1	4.14	7	36.18	10.2
4	9.9	8.3	2.85	6.51	1.03	5	3.55	6.8	26.54	9.7
5	9.9	8.3	2.85	6.51	1.02	5	3.22	6.7	20.03	9.3

Table 22. $\sigma_{\max-NORM}$ **for n =10**

x / n_1	0.01	Δn_{EQ}	0.1	Δn_{EQ}	0.5	Δn_{EQ}	0.9	Δn_{EQ}	0.99	Δn_{EQ}
1	9.9	9.3	2.86	7.52	1.15	6.2	6.53	8.7	70.18	12.1
2	9.9	9.3	2.86	7.52	1.09	6.1	5.09	8.3	50.18	11.6
3	9.9	9.3	2.86	7.51	1.05	6.1	4.14	8	36.19	11.2
4	9.9	9.3	2.85	7.51	1.03	6	3.55	7.8	26.54	10.7
5	9.9	9.3	2.85	7.51	1.02	6	3.22	7.7	20.03	10.3

Table 23. $\sigma_{\max-NORM}$ **for n =11**

x / n_1	0.01	Δn_{EQ}	0.1	Δn_{EQ}	0.5	Δn_{EQ}	0.9	Δn_{EQ}	0.99	Δn_{EQ}
1	9.9	10.1	2.86	8.52	1.15	7.2	6.53	9.7	70.18	13.1
2	9.9	10.1	2.86	8.52	1.1	7.1	5.09	9.3	50.18	12.6
3	9.9	10.1	2.86	8.51	1.05	7.1	4.14	9	36.18	12.2
4	9.9	10.1	2.85	8.51	1.03	7	3.56	8.8	26.53	11.7
5	9.9	10.1	2.85	8.51	1.01	7	3.22	8.7	20.03	11.3
6	9.9	10.1	2.85	8.51	1.01	7	3.04	8.6	15.8	11

Table 24. $\sigma_{\max-NORM}$ **for n =12**

x / n_1	0.01	Δn_{EQ}	0.1	Δn_{EQ}	0.5	Δn_{EQ}	0.9	Δn_{EQ}	0.99	Δn_{EQ}
1	9.9	11.3	2.86	9.52	1.15	8.2	6.53	10.7	70.18	14.1
2	9.9	11.3	2.86	9.52	1.1	8.1	5.09	10.3	50.18	13.6
3	9.9	11.3	2.86	9.51	1.05	8.1	4.14	10	36.19	13.2
4	9.9	11.3	2.85	9.51	1.03	8	3.56	9.8	26.53	12.7
5	9.9	11.3	2.85	9.51	1.02	8	3.22	9.7	20.03	12.3
6	9.9	11.3	2.85	9.51	1.01	8	3.04	9.6	15.8	12

APPENDIX C. $\sigma_{max-NORM}$ OF A DUAL LADDER DAC WITH BUFFER RESISTORS

Table 25. The minimum $\sigma_{max-NORM}$ for n = 4, n_1 =2

x	a_1	a_2	a_3	Min $\sigma_{max-NORM}$
0.1	0.1	0.19	0.71	8.87
0.2	0.2	0.19	0.61	8.84
0.3	0.3	0.19	0.51	8.84
0.4	0.3	0.19	0.51	8.81
0.5	0.4	0.19	0.41	8.76
0.6	0.5	0.19	0.31	8.77
0.7	0.6	0.19	0.21	8.8
0.8	0.7	0.19	0.11	8.89
0.9	0.7	0.19	0.11	8.89

Table 26. The minimum $\sigma_{max-NORM}$ for n = 5, n_1 =2

x	a_1	a_2	a_3	Min $\sigma_{max-NORM}$
0.1	0.1	0.19	0.71	17.8
0.2	0.2	0.19	0.61	17.7
0.3	0.3	0.19	0.51	17.7
0.4	0.3	0.19	0.51	17.6
0.5	0.4	0.19	0.41	17.6
0.6	0.5	0.19	0.31	17.5
0.7	0.6	0.19	0.21	17.6
0.8	0.7	0.19	0.11	17.8
0.9	0.7	0.19	0.11	17.8

Table 27. The minimum $\sigma_{max-NORM}$ for n = 6, n_1 =2

x	a_1	a_2	a_3	Min $\sigma_{max-NORM}$
0.1	0.1	0.19	0.71	35.5
0.2	0.2	0.19	0.61	35.4
0.3	0.3	0.19	0.51	35.4
0.4	0.3	0.19	0.51	35.2
0.5	0.4	0.19	0.41	35.1
0.6	0.5	0.19	0.31	35.1
0.7	0.6	0.19	0.21	35.2
0.8	0.7	0.19	0.11	35.6
0.9	0.7	0.19	0.11	35.6

Table 28. The minimum $\sigma_{max-NORM}$ for n = 6, n_1 =3

x	a_1	a_2	a_3	Min $\sigma_{max-NORM}$
0.1	0.1	0.09	0.81	34
0.2	0.2	0.09	0.71	34
0.3	0.3	0.09	0.61	34
0.4	0.4	0.09	0.51	34
0.5	0.5	0.09	0.41	34
0.6	0.5	0.09	0.41	34
0.7	0.6	0.09	0.31	34
0.8	0.7	0.09	0.21	34
0.9	0.8	0.09	0.11	34

Table 29. The minimum $\sigma_{max-NORM}$ for n = 7, n_1 =2

x	a_1	a_2	a_3	Min $\sigma_{max-NORM}$
0.1	0.1	0.19	0.71	71
0.2	0.2	0.19	0.61	70.8
0.3	0.3	0.19	0.51	70.7
0.4	0.3	0.19	0.51	70.4
0.5	0.4	0.19	0.41	70.2
0.6	0.5	0.19	0.31	70.2
0.7	0.6	0.19	0.21	70.4
0.8	0.7	0.19	0.11	71.1
0.9	0.7	0.19	0.11	71.2

Table 30. The minimum $\sigma_{max-NORM}$ for n = 7, n_1 =3

x	a_1	a_2	a_3	Min $\sigma_{max-NORM}$
0.1	0.1	0.09	0.81	68
0.2	0.2	0.09	0.71	68
0.3	0.3	0.09	0.61	68
0.4	0.4	0.09	0.51	68
0.5	0.5	0.09	0.41	68
0.6	0.5	0.09	0.41	68
0.7	0.6	0.09	0.31	68
0.8	0.7	0.09	0.21	68
0.9	0.8	0.09	0.11	68

Table 31. The minimum $\sigma_{max-NORM}$ for n = 8, n_1 =2

x	a_1	a_2	a_3	Min $\sigma_{max-NORM}$
0.1	0.1	0.19	0.71	142.1
0.2	0.2	0.19	0.61	141.5
0.3	0.3	0.19	0.51	141.4
0.4	0.3	0.19	0.51	140.9
0.5	0.4	0.19	0.41	140.4
0.6	0.5	0.19	0.31	140.3
0.7	0.6	0.19	0.21	140.7
0.8	0.7	0.19	0.11	142.2
0.9	0.7	0.19	0.11	142.4

Table 32. The minimum $\sigma_{max-NORM}$ for n = 8, n_1 =3

x	a_1	a_2	a_3	Min $\sigma_{max-NORM}$
0.1	0.1	0.09	0.81	135.9
0.2	0.2	0.09	0.71	135.8
0.3	0.3	0.09	0.61	135.8
0.4	0.4	0.09	0.51	135.9
0.5	0.5	0.09	0.41	136
0.6	0.5	0.09	0.41	136.1
0.7	0.6	0.09	0.31	136.9
0.8	0.7	0.09	0.21	135.8
0.9	0.8	0.09	0.11	135.8

Table 33. The minimum $\sigma_{max-NORM}$ for n = 8, n_1 =4

x	a_1	a_2	a_3	Min $\sigma_{max-NORM}$
0.1	0.1	0.09	0.81	132.6
0.2	0.2	0.09	0.71	132.6
0.3	0.3	0.09	0.61	132.7
0.4	0.4	0.09	0.51	132.9
0.5	0.5	0.09	0.41	133.2
0.6	0.6	0.09	0.31	133.7
0.7	0.6	0.09	0.31	133.8
0.8	0.7	0.09	0.21	133.9
0.9	0.8	0.09	0.11	134.1

Table 34. The minimum $\sigma_{max-NORM}$ for n = 9, n_1 =2

x	a_1	a_2	a_3	Min $\sigma_{max-NORM}$
0.1	0.1	0.19	0.71	284.2
0.2	0.2	0.19	0.61	283
0.3	0.3	0.19	0.51	283
0.4	0.3	0.19	0.51	281.8
0.5	0.4	0.19	0.41	280.8
0.6	0.5	0.19	0.31	280.7
0.7	0.6	0.19	0.21	281.5
0.8	0.7	0.19	0.11	284.5
0.9	0.7	0.19	0.11	284.8

Table 35. The minimum $\sigma_{max-NORM}$ for n = 9, n_1 =3

x	a_1	a_2	a_3	Min $\sigma_{max-NORM}$
0.1	0.1	0.09	0.81	271.9
0.2	0.2	0.09	0.71	271.6
0.3	0.3	0.09	0.61	271.6
0.4	0.4	0.09	0.51	271.7
0.5	0.5	0.09	0.41	272
0.6	0.5	0.09	0.41	272.2
0.7	0.6	0.09	0.31	271.9
0.8	0.7	0.09	0.21	271.7
0.9	0.8	0.09	0.11	271.7

Table 36. The minimum $\sigma_{max-NORM}$ for n = 9, n_1 =4

x	a_1	a_2	a_3	Min $\sigma_{max-NORM}$
0.1	0.1	0.09	0.81	265.1
0.2	0.2	0.09	0.71	265.2
0.3	0.3	0.09	0.61	265.4
0.4	0.4	0.09	0.51	265.8
0.5	0.5	0.09	0.41	266.4
0.6	0.6	0.09	0.31	267.4
0.7	0.6	0.09	0.31	267.6
0.8	0.7	0.09	0.21	267.8
0.9	0.8	0.09	0.11	268.3

Table 37. The minimum $\sigma_{max-NORM}$ for n = 10, n_1 =2

x	a_1	a_2	a_3	Min $\sigma_{max-NORM}$
0.1	0.1	0.19	0.71	568.3
0.2	0.2	0.19	0.61	566
0.3	0.3	0.19	0.51	565.7
0.4	0.3	0.19	0.51	563.6
0.5	0.4	0.19	0.41	561.7
0.6	0.5	0.19	0.31	561.4
0.7	0.6	0.19	0.21	563
0.8	0.7	0.19	0.11	568.9
0.9	0.7	0.19	0.11	569.7

Table 38. The minimum $\sigma_{max-NORM}$ for n = 10, n_1 =3

x	a_1	a_2	a_3	Min $\sigma_{max-NORM}$
0.1	0.1	0.09	0.81	543.7
0.2	0.2	0.09	0.71	543.2
0.3	0.3	0.09	0.61	543.1
0.4	0.4	0.09	0.51	543.4
0.5	0.5	0.09	0.41	544.1
0.6	0.5	0.09	0.41	544.4
0.7	0.6	0.09	0.31	543.8
0.8	0.7	0.09	0.21	543.4
0.9	0.8	0.09	0.11	543.3

Table 39. The minimum $\sigma_{max-NORM}$ for n = 10, n_1 =4

x	a_1	a_2	a_3	Min $\sigma_{max-NORM}$
0.1	0.1	0.09	0.81	530.3
0.2	0.2	0.09	0.71	530.4
0.3	0.3	0.09	0.61	530.8
0.4	0.4	0.09	0.51	531.5
0.5	0.5	0.09	0.41	532.7
0.6	0.6	0.09	0.31	534.7
0.7	0.6	0.09	0.31	535.2
0.8	0.7	0.09	0.21	535.7
0.9	0.8	0.09	0.11	536.5

Table 40. The minimum $\sigma_{max-NORM}$ for n = 10, n_1 =5

x	a_1	a_2	a_3	Min $\sigma_{max-NORM}$
0.1	0.1	0.09	0.81	531.5
0.2	0.2	0.09	0.71	532.1
0.3	0.3	0.09	0.61	532.9
0.4	0.4	0.09	0.51	534
0.5	0.5	0.09	0.41	535.4
0.6	0.5	0.09	0.41	536.9
0.7	0.6	0.09	0.31	536.7
0.8	0.7	0.09	0.21	536.8
0.9	0.8	0.09	0.11	537.2

BIBLIOGRAPHY

Boylston, L. E. et al. (2002). Enhacing performance in interpolating resistor string DACs, *Proceedings of the 45th IEEE Midwest Symposium on Circuits and Systems,* 2, 541–544.

Pelgrom, M. J. M. et al. (1989). Matching properties of MOS transistors. *IEEE J. Solid-State Circuits,* 24(5), 1433-1439.

Pelgrom, M. J. M. (1990). A 10-b 50-MHz CMOS D/A converter with 75-Ω buffer. *IEEE Journal of Solid State Circuits*, 25(6), 1347–1352.

Maloberti, F. et al. (1996). Power consumption optimization of 8 bit, 2MHz voltage scaling subranging CMOS 0.5-μm dac. *Proceeding of the Third IEEE International Conference on Electronics, Circuits, and Systems.* 2, 1162–1165.

Plassche, R. van de (2003). *CMOS Integrated Analog-to-Digital and Digital-to-Analog Converters*. Boston: Kluwer Academic.

Rivoir, R., Maloberti, F. and Torelli, G.P. (1997). Digital to analog converter with dual resistor string. *U.S. Patent No. 5,703,588*.

Hastings, A. (2000). *The Art of Analog Layout*. New Jersey: Prentice Hall.

He, C. et al. (2004). Nth order circular symmetry pattern and hexagonal tessellation: two new layout techniques canceling non-linear gradient. *IEEE International Symposium on Circuits and Systems*, 1, 237-240.

He, C. et al. (2006). New layout strategies with improves matching performance. *Analog integrated circuits and signal processing*, 49(3), 281-289.

Lane, W. and Wrixon, G. (1989). The design of thin-film polysilicon resistors for analog IC applications. *IEEE Transactions on Electron Devices*, 36(4), 738–744.

Lin, Y. and Geiger, R. (2001). Resistor layout techniques for enhancing yield in ratio-critical monolithic applications. *Proceedings of the 44th IEEE Midwest Symposium Circuits and Systems*, 1, 259–262.

ACKNOWLEDGEMENTS

First and foremost, I would like to thank my adviser Dr. Randall Geiger who has inspired my work from the beginning. His intellectual support, ideas, patience and cheerfulness in addressing my questions have been encouraging and helped me complete this research.

I would also like to thank my committee members Dr. Chen Degang and Dr. Tien Nguyen for their helpful discussion and comments.

My special thanks go to my parents, my husband and my lovely son. Without their support and their love, I would not have been able to complete this work.